SHANDONG UNIVERSITY

Probing neutron skin thickness with parity-violating electron scattering

Reference: D. Adhikari et al., (PREX Col.) PRL 126, 172502 (2021)

Jinlong Zhang (张金龙)

Shandong University

October 21, 2021

Credits:

- Much of the work is done by other dedicated people as part of the PREX/CREX collaboration
- I borrowed a lot of plots from talks of my collaborators, especially C. Gal.

Parity violating in weak interaction

The Nobel Prize in Physics 1957

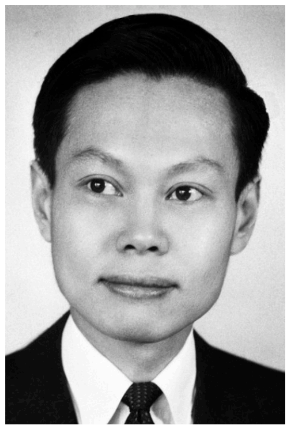

Photo from the Nobel Foundation archive.

Chen Ning Yang

Prize share: 1/2

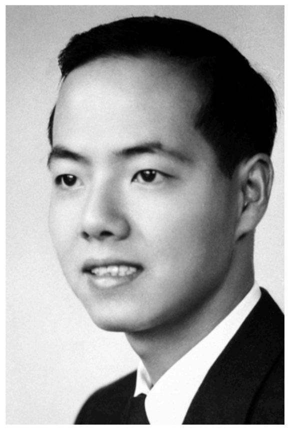

Photo from the Nobel Foundation archive.

Tsung-Dao (T.D.) Lee

Prize share: 1/2

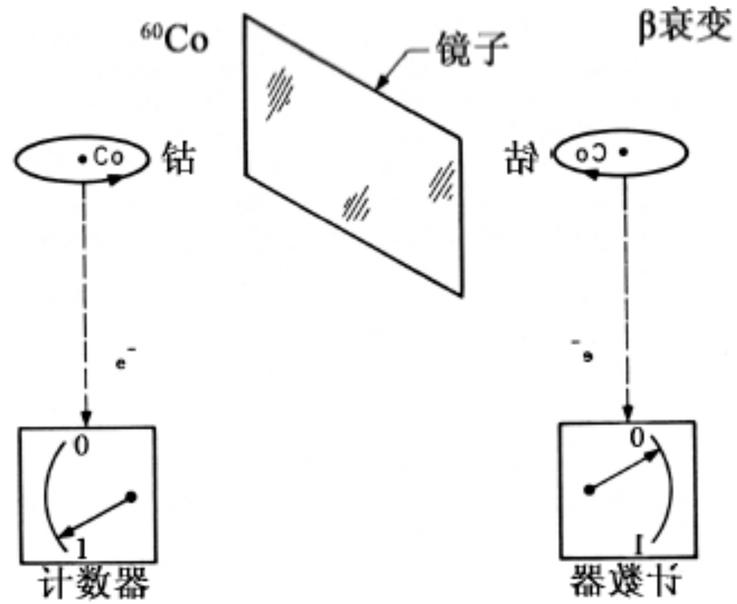

Chien-Shiung Wu
Forever Stamps
U.S. Postal Service

The Nobel Prize in Physics 1957 was awarded jointly to Chen Ning Yang and Tsung-Dao (T.D.) Lee "for their penetrating investigation of the so-called parity laws which has led to important discoveries regarding the elementary particles."

Chien-Shiung Wu
Chien-Shiung Wu (1912-1997) was one of the most influential nuclear physicists of the 20th century. During a career that spanned more than 40 years in a field dominated by men, she established herself as the authority on conducting precise and accurate research to test fundamental theories of physics. Art Director Ethel Kessler designed the stamp with original art by Kam Mak.

NobelPrize.org

usps.com

Parity Violating Electron Scattering

Flip spin of electrons and look for difference in scattering rate

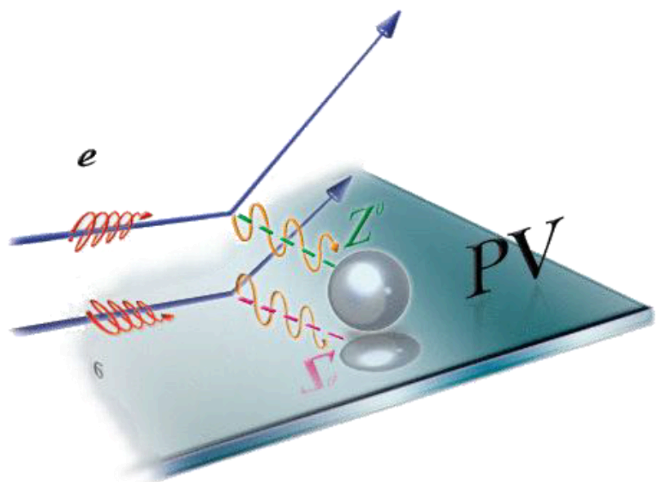

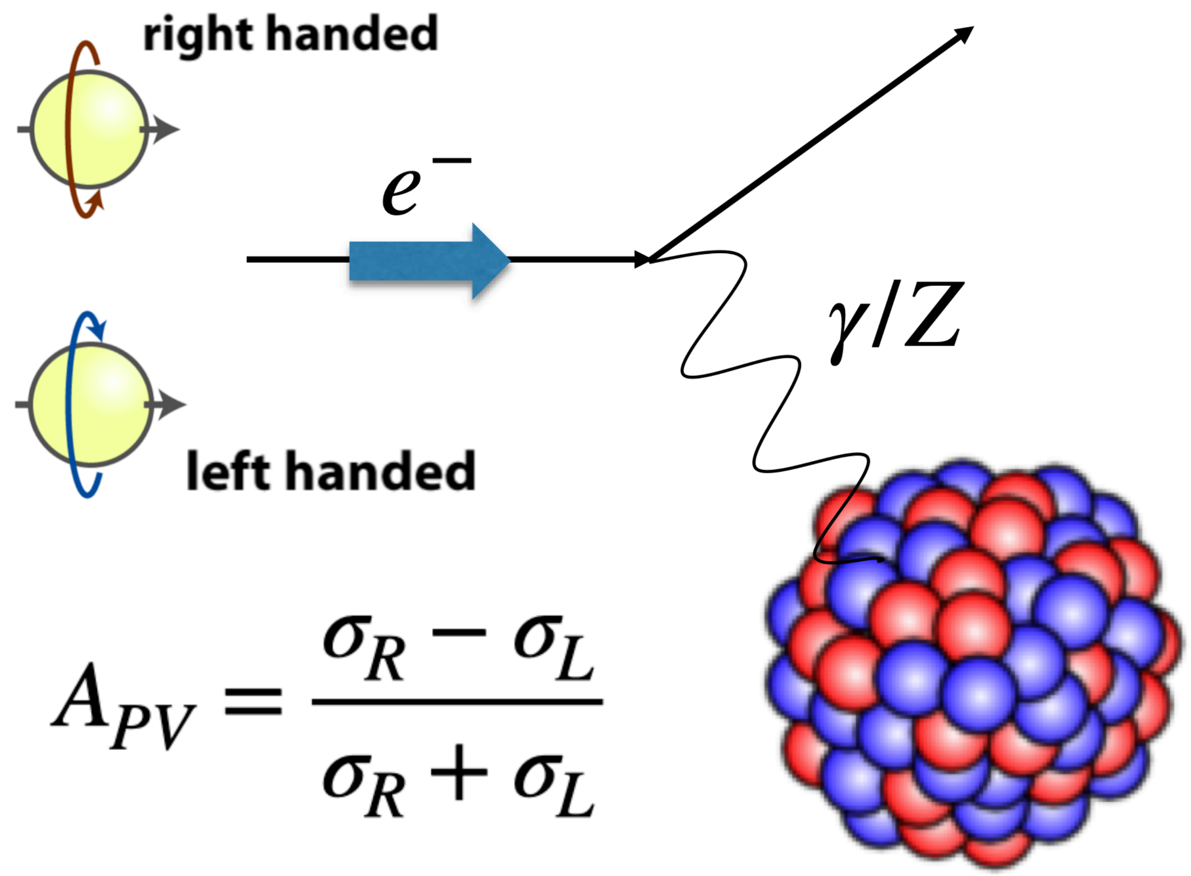

$$A_{PV} = \frac{\sigma_R - \sigma_L}{\sigma_R + \sigma_L}$$

$$A_{PV} = \frac{\sigma_R - \sigma_L}{\sigma_R + \sigma_L} \sim$$

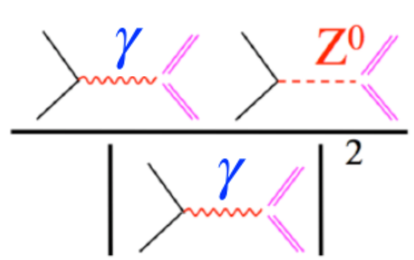

$$\propto \frac{|M_Z|}{|M_\gamma|} \approx \frac{G_F Q^2 Q_W}{4\pi\alpha\sqrt{2}Z} \frac{F_W(Q^2)}{F_{ch}(Q^2)} \sim 10^{-4} \times Q^2$$

Clean and theoretically easy interpretation, but very challenging!

Parity Violating Electron Scattering

PVES Landscape

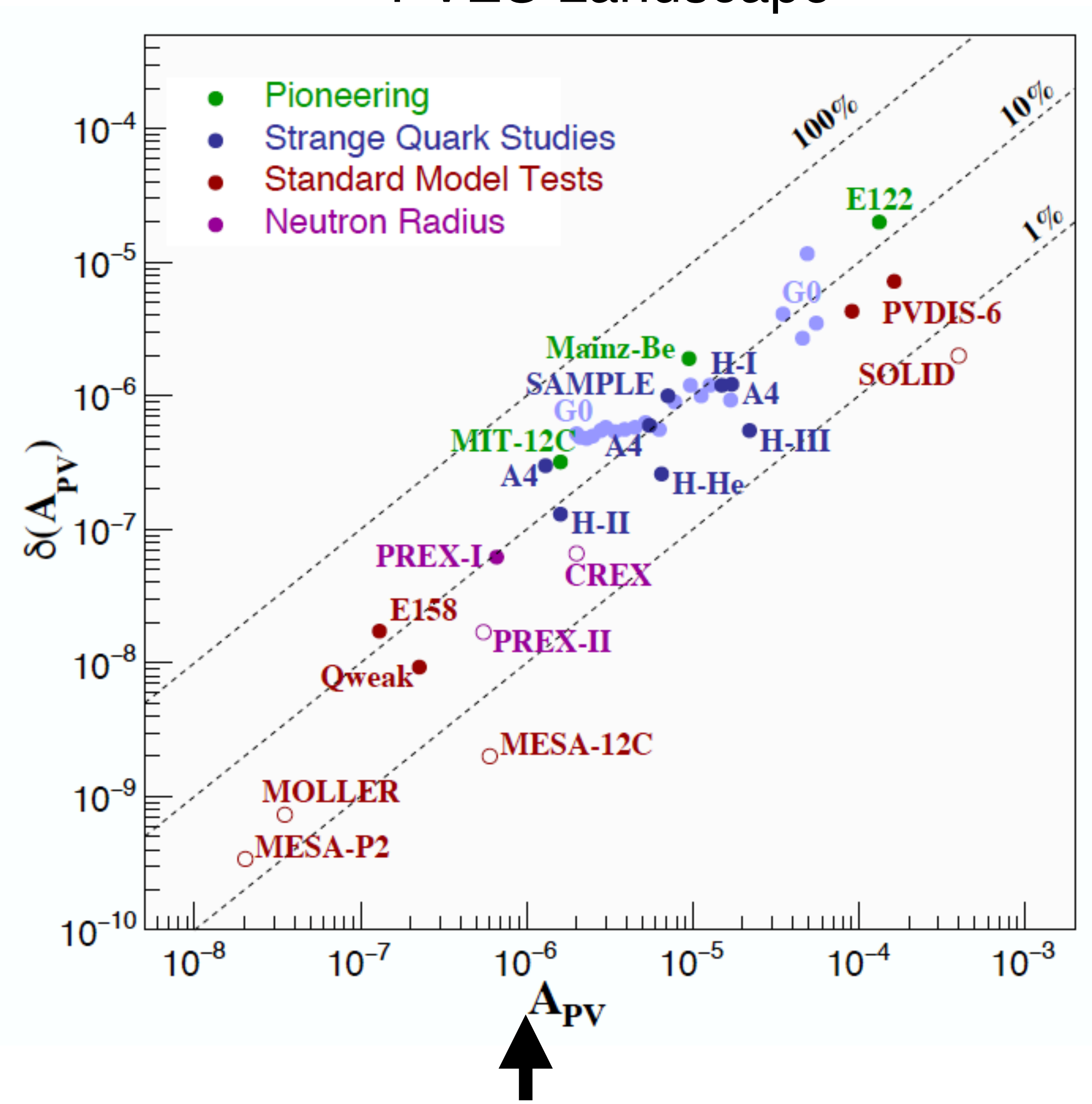

1,000,000 vs. 1,000,001 ppm (part per million)

- PVES has a long history of pushing the limits of precision and discovery
  - E122: (ΔA=10 ppm) 1978
    - pioneering experiment (already had most of the features of modern PVES experiments)
  - Strange form factor
    - G0, HAPPEX
  - Standard Model Tests
    - E158, PVDIS, Qweak
  - **Nuclear structure / neutron skin**
    - **PREX, PREX-II, CREX**
  - Future:
    - MOLLER, P2, SoLID

High statistics and excellent systematics control

What's the size of nucleus?

- Proton distribution:
  - Owing to the electric charge, this has been accurately measured for many atomic nuclei
- Neutron distribution: poorly known
  - Primarily from hadron experiments (pN, HIC, Rare Isotope, electric dipole polarizability, etc), model dependent
  - Parity-violating electron scattering: via the weak charge

Charge type	Proton	Neutron
Electric	1	0
Weak	~0.07	-1

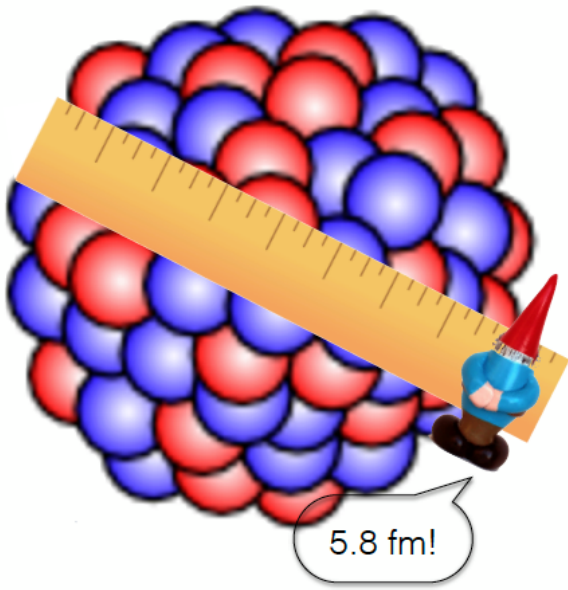

Weak interaction sees neutrons

Neutron Skin

J. Phys. G: Nucl. Part. Phys. 46 (2019) 093003

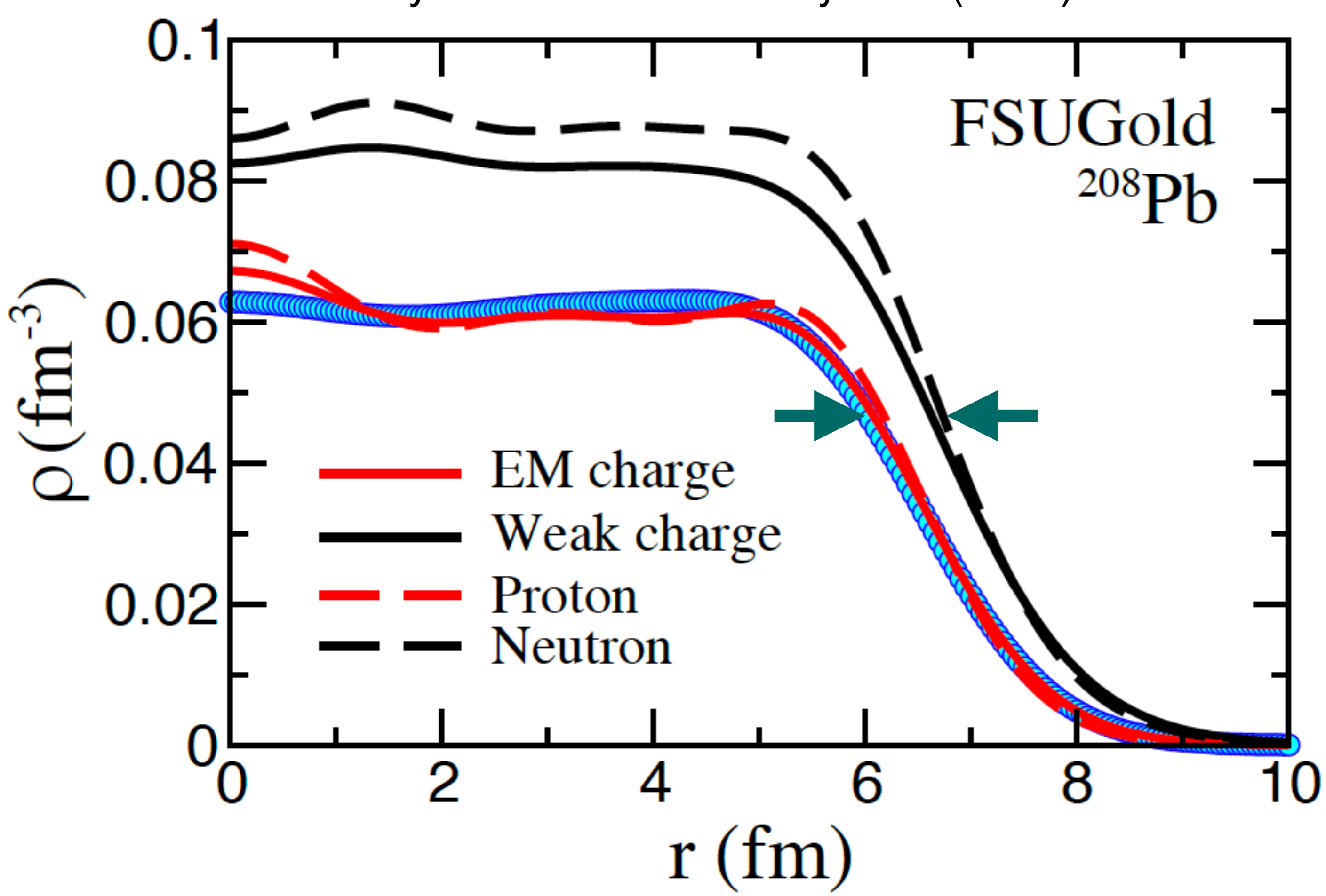

- For N=Z: the neutron and proton density distributions are expected to have a similar shape
- For N>>Z, the excess neutrons are pushed out to the periphery forming a **neutron skin**

Neutron skin: Difference between **root-mean-squared** radii of neutron and proton.

$$\Delta r_{np} = R_n - R_p = \sqrt{<r_n^2>} - \sqrt{<r_p^2>}$$

Neutron Skin and Symmetry Energy

Symmetry energy $S(\rho)$: energy penalty for breaking N=Z symmetry

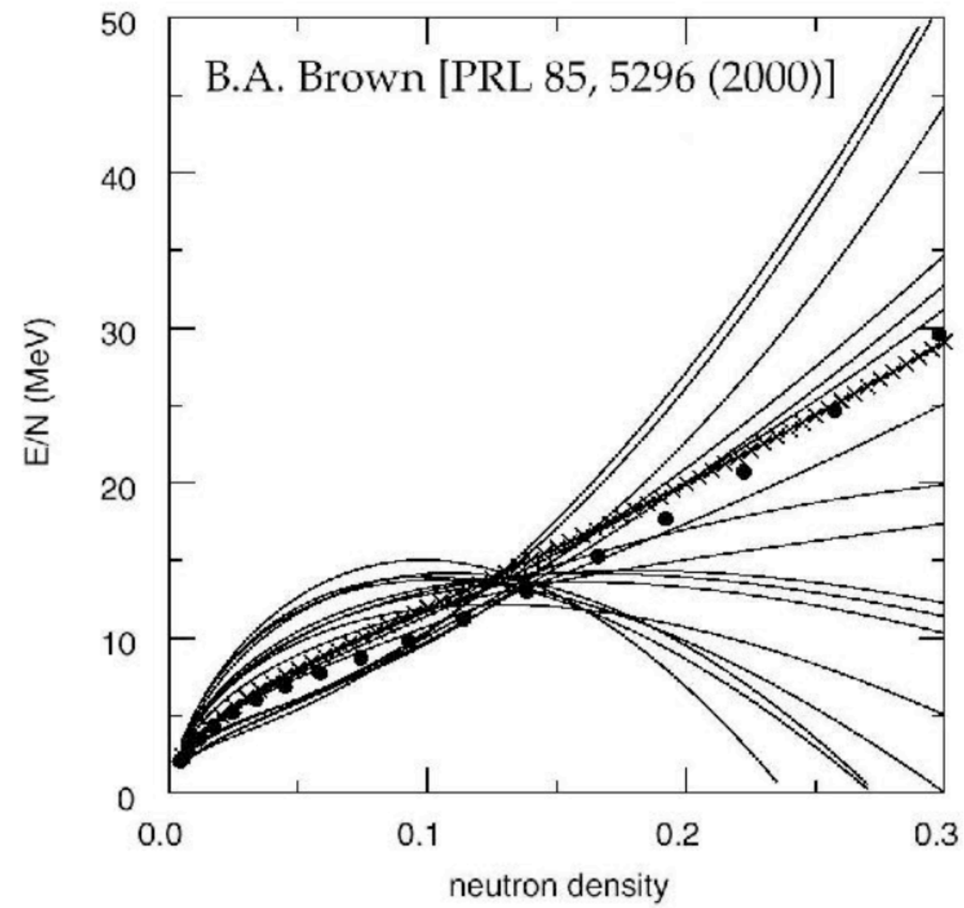

FIG. 2. The neutron EOS for 18 Skyrme parameter sets. The filled circles are the Friedman-Pandharipande (FP) variational calculations and the crosses are SkX. The neutron density is in units of neutron/fm^3.

Slope of the symmetry energy L:

$$L \propto \frac{\partial S(\rho)}{\partial \rho}\Big|_{\rho_0}$$

Symmetry energies are different in the inner core (high density) and outer core (low density)

The extent of the neutron skin in a neutron rich nucleus is the result of balance between the surface tension and the slope of the symmetry energy.

Neutron Skin and Symmetry Energy

Mean-Field predictions show a correlation between neutron skin of a heavy nucleus, Δr_{np}, and the density slope of the symmetry energy.

X. Roca-Maza (et al.) PRL 106 (2011) 252501

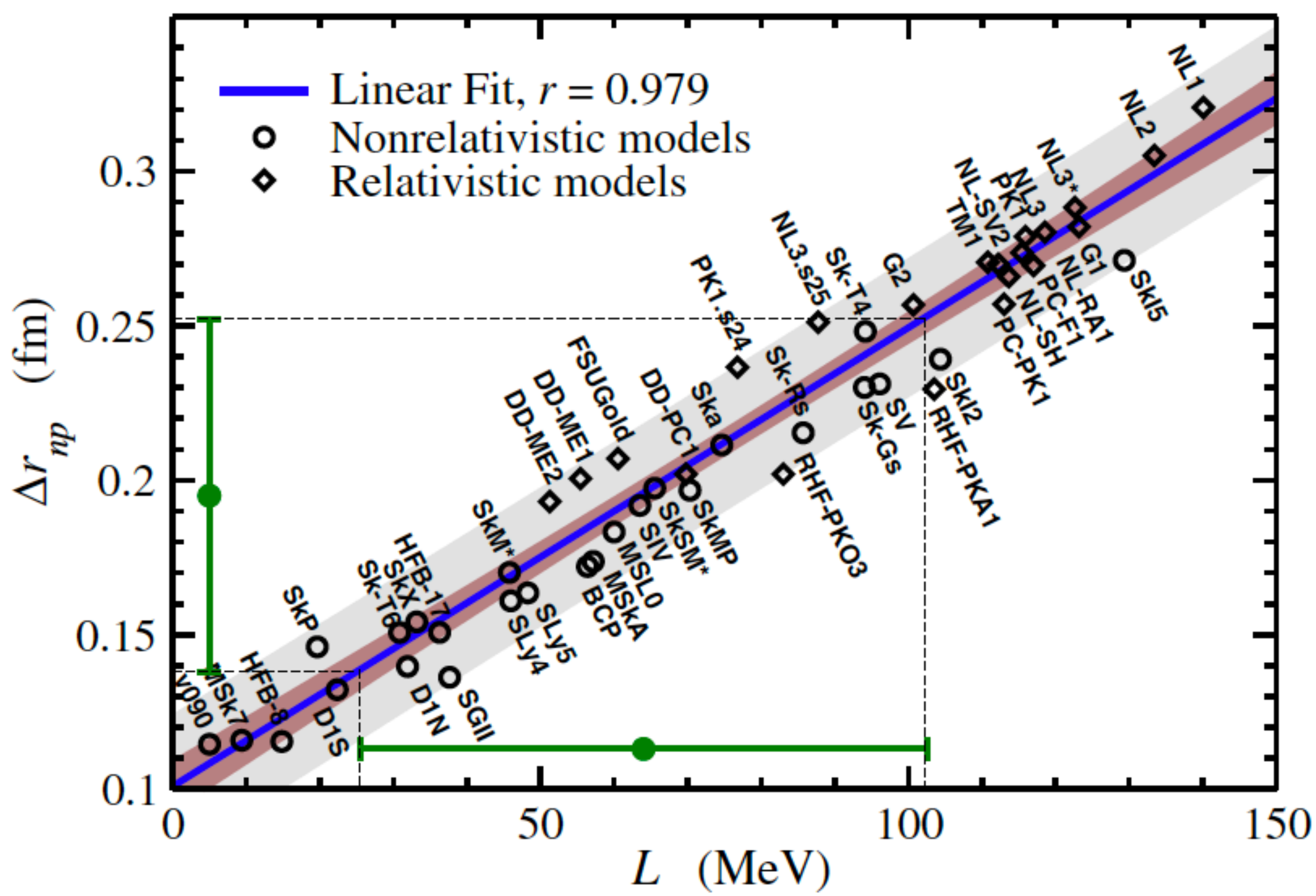

Δr_{np} calibrates the Equation of State of neutron rich matter, determining L constrains and guides models needed for heavy nuclei

Neutron Skin and Neutron Star

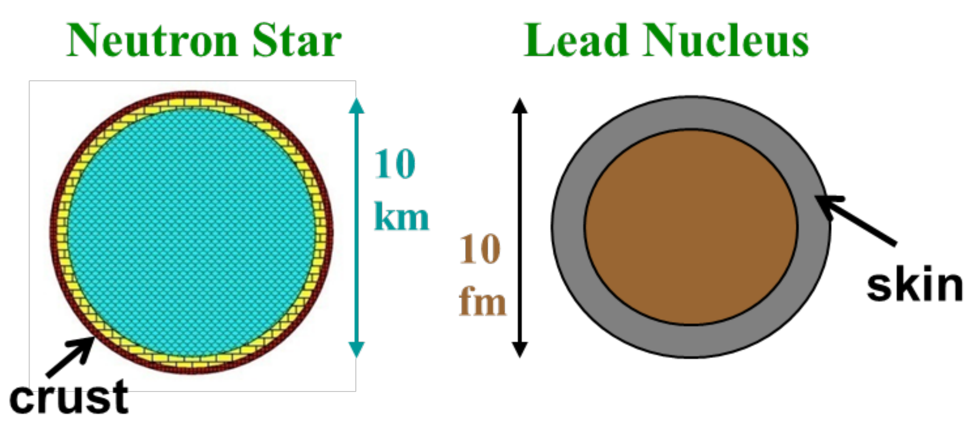

Farrukh J. Fattoyev - Jan 24, 2018 JLab seminar

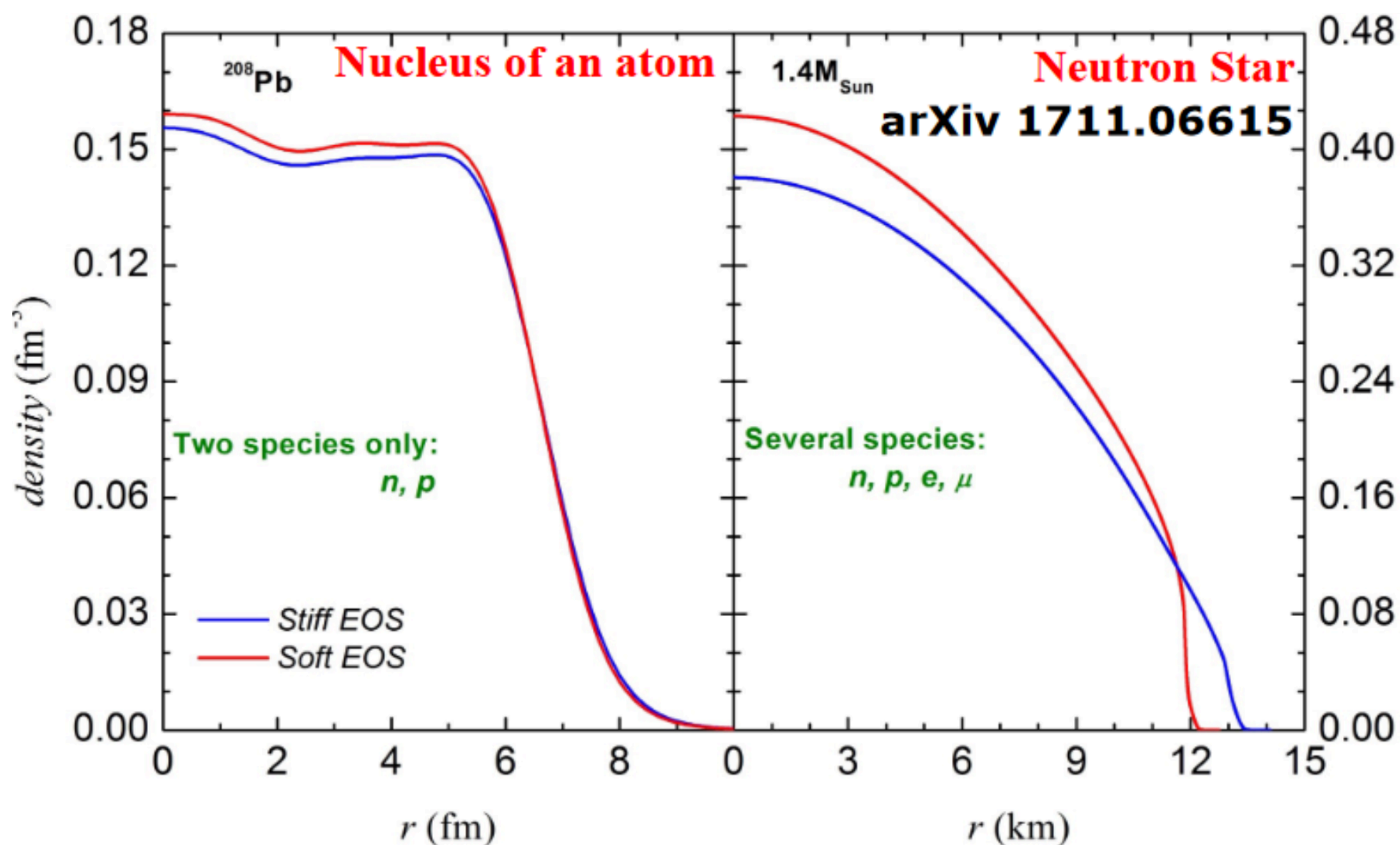

A “typical” neutron star has a
mass of ~1.5 solar masses, M⊙,
radius of ~10 km,
density as high as 5-10 times that of lab nuclei

- In spite of the 18 orders of magnitude size difference, heavy nucleus and neutron star are both described with the nuclear Equation of State
  - Both strongly correlated with the slope of the symmetry energy L

Constraints deduced from Binary Neutron Stars

Binary Neutron Stars Merger

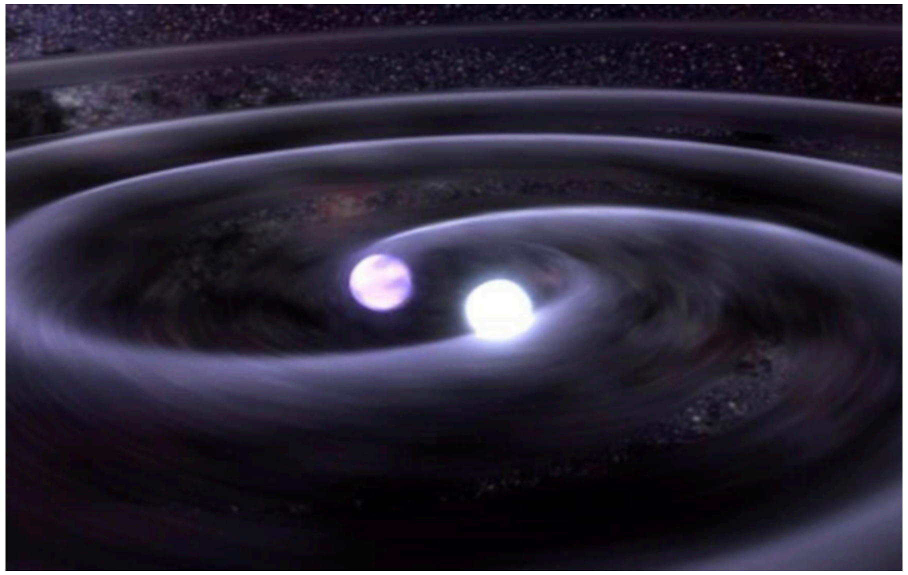

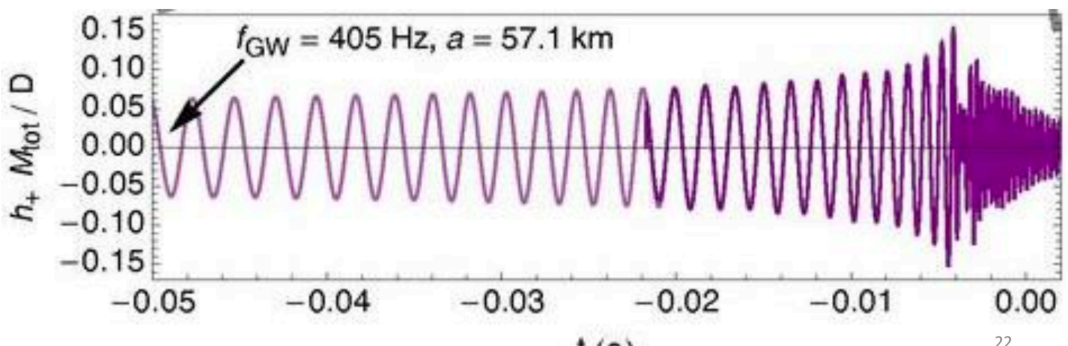

Image Credit: Jocelyn Read

J. Phys. G: Nucl. Part. Phys. 46 (2019) 093003

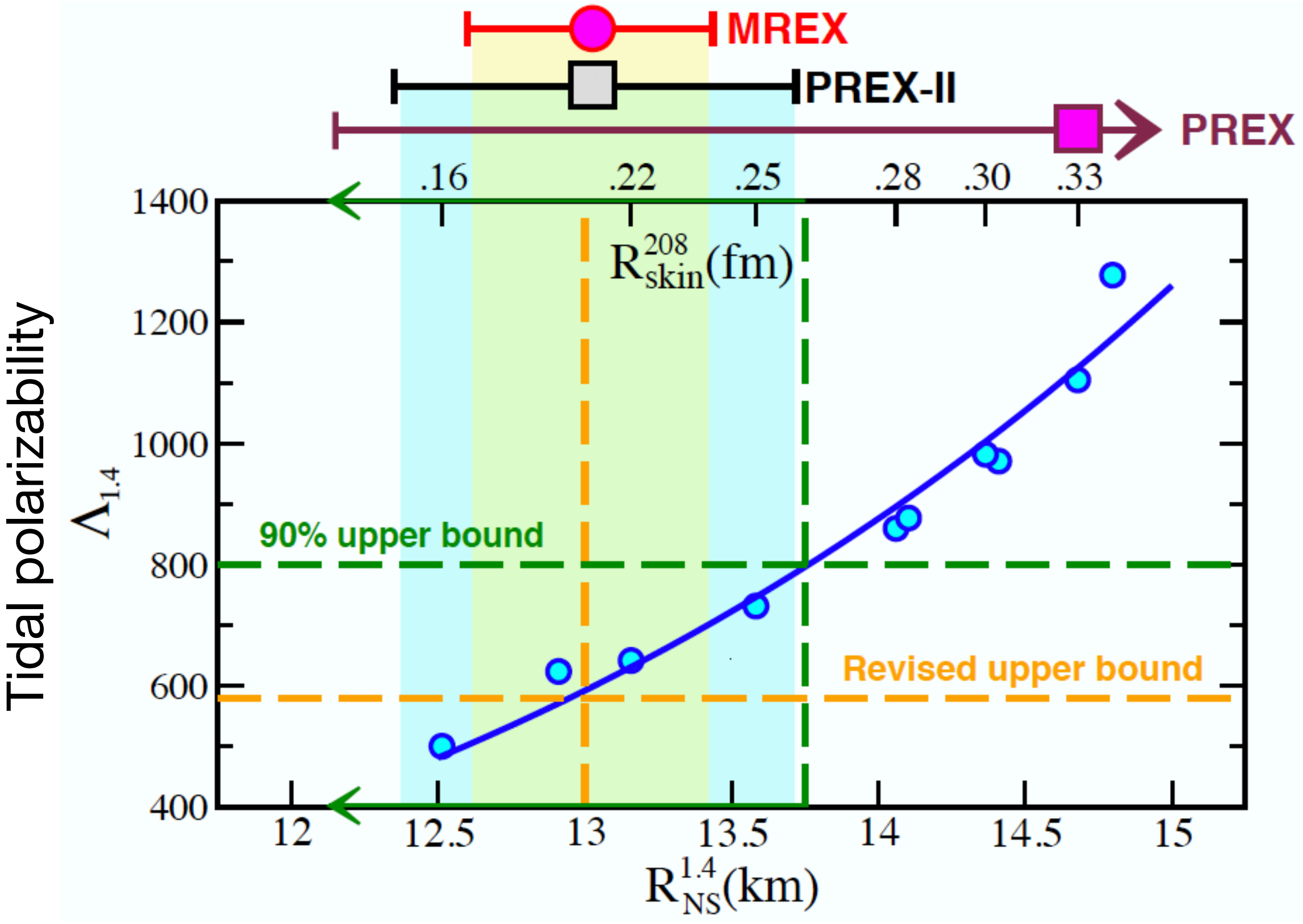

The induced quadrupole deformation will advance the orbit in this case and change the phase of rotation!

Binary Neutron Stars merger significantly limits the phase space for the neutron skin

Choice of Nuclei Target

Stable and Least theoretical uncertainties

- Doubly-magic; Neutron excess; First excited state far from elastic

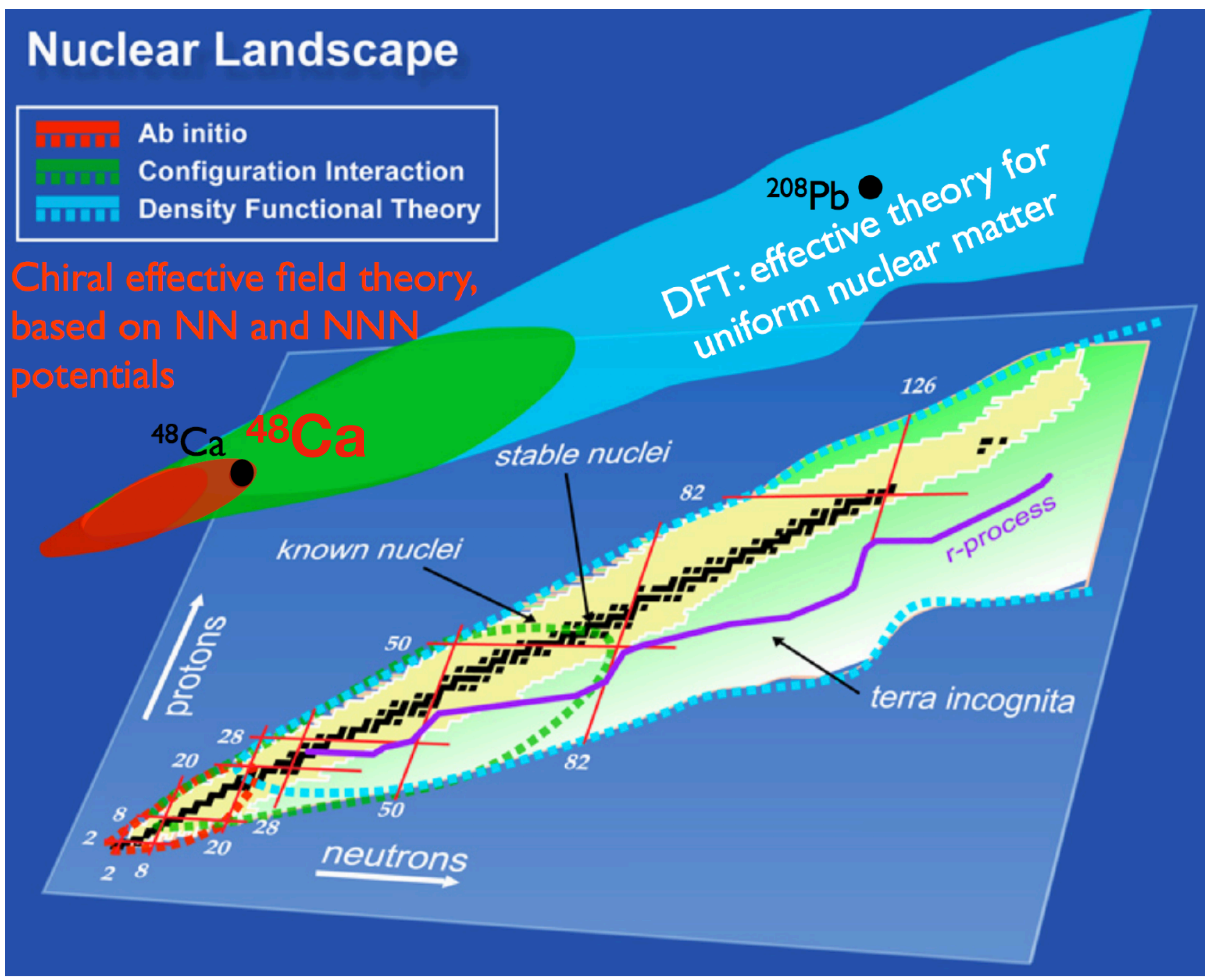

PREX

^{208}Pb:

- in realm of uniform nuclear matter & Density Functional Theory
- serves as terrestrial laboratory to test neutron star structure

CREX

^{48}Ca:

- "*ab initio*" (exact microscopic) calculations of R_{skin} for ^{48}Ca have recently been available.

  G. Hagen et al., *Nature Physics 12, 186(2016).*

- bridge between "*ab initio*" models and effective theory (DFT)

ab initio Calculation

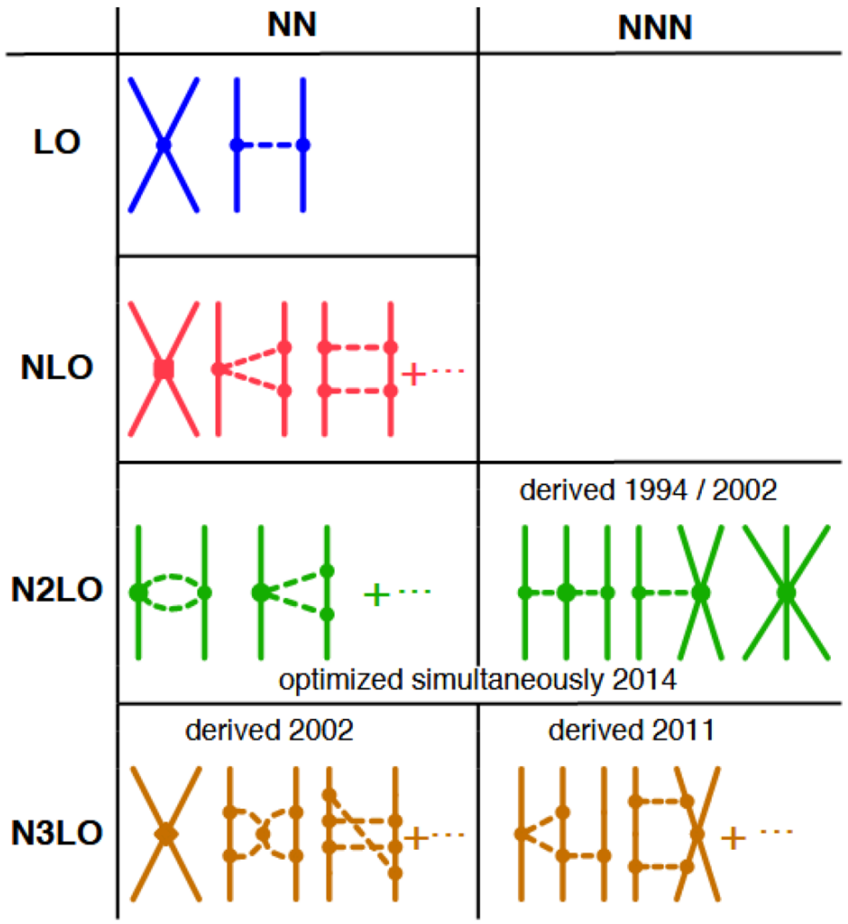

G. Hagen et al., *Nature Physics 12, 186(2016).*

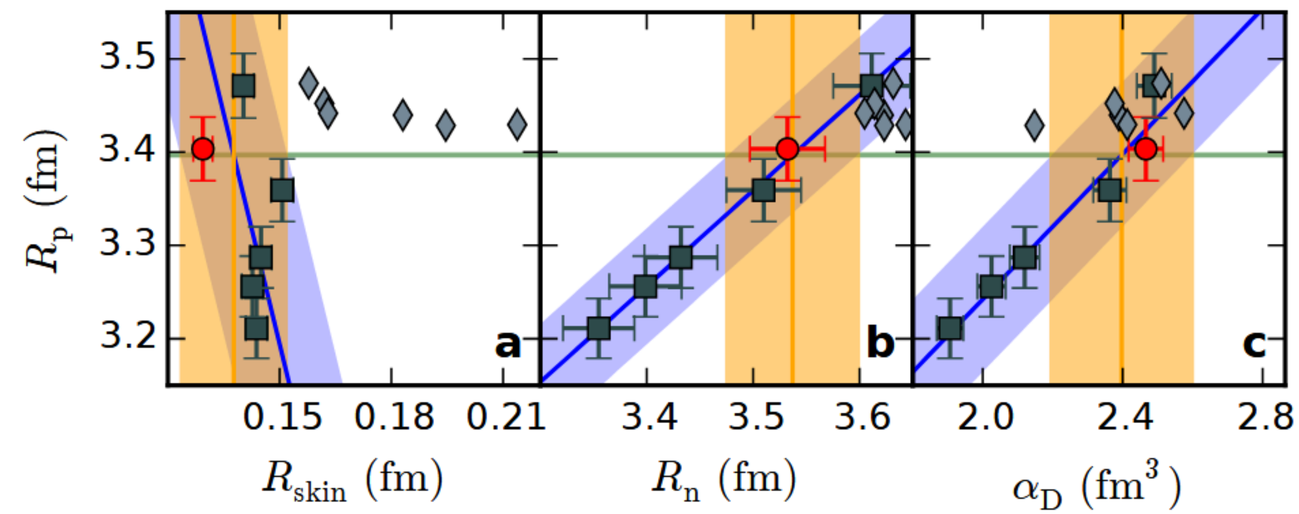

Figure 1 | Predictions for observables related to the neutron distribution in ^{48}Ca. a, the neutron skin R_{skin}; **b**, the point-neutron radius R_n; and **c**, the electric dipole polarizability α_D – all versus the point-proton radius R_p. The *ab initio* predictions with $NNLO_{sat}$ (dots) and chiral interactions of ref. 28 (squares) are compared to the DFT results with the energy density functionals SkM*, SkP, SLy4, SV-min, UNEDF0, and UNEDF1[19] (diamonds). The theoretical error bars are indicated. The blue line represents a linear fit to the data, with theoretical uncertainties shown by a blue band. The horizontal green line marks the experimental value of R_p that puts a constraint on the ordinate (orange band).

- Coupled cluster method: solve the quantum nuclear many-body problem; Nuclear forces based on chiral effective field theory.

- Predicted a smaller ^{48}Ca neutron skin thickness than DFT

- Extra important need for CREX result.

From A_{PV} to Neutron Skin

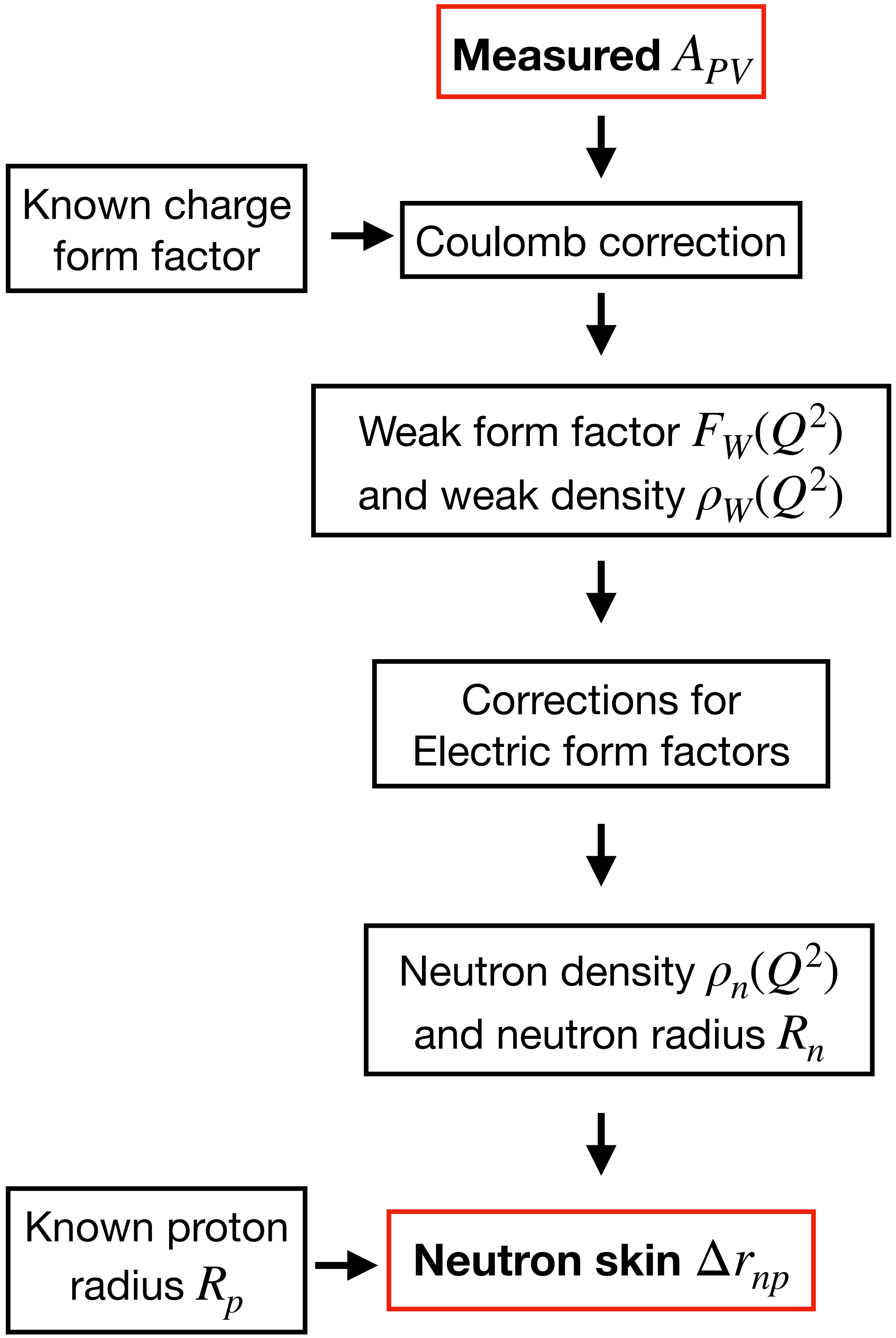

X. Roca-Maza (et al.) PRL 106 (2011) 252501

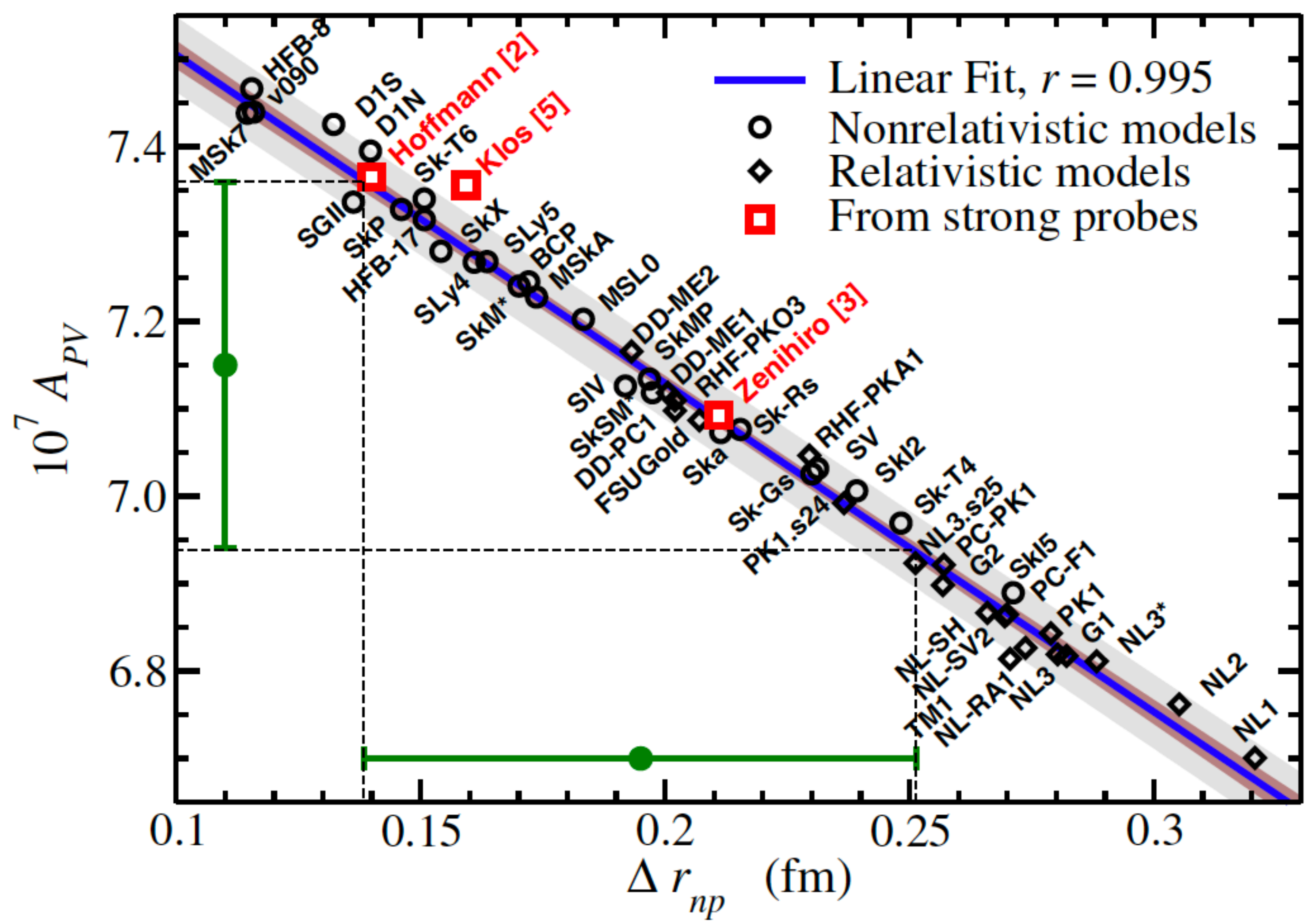

Robust correlation between ^{208}Pb A_{PV} and the neutron skin over existing nuclear structure models

Different neuron skin thickness from different models, **experimental data needed.**

Continuous Electron Beam Accelerator Facility at Jefferson Lab

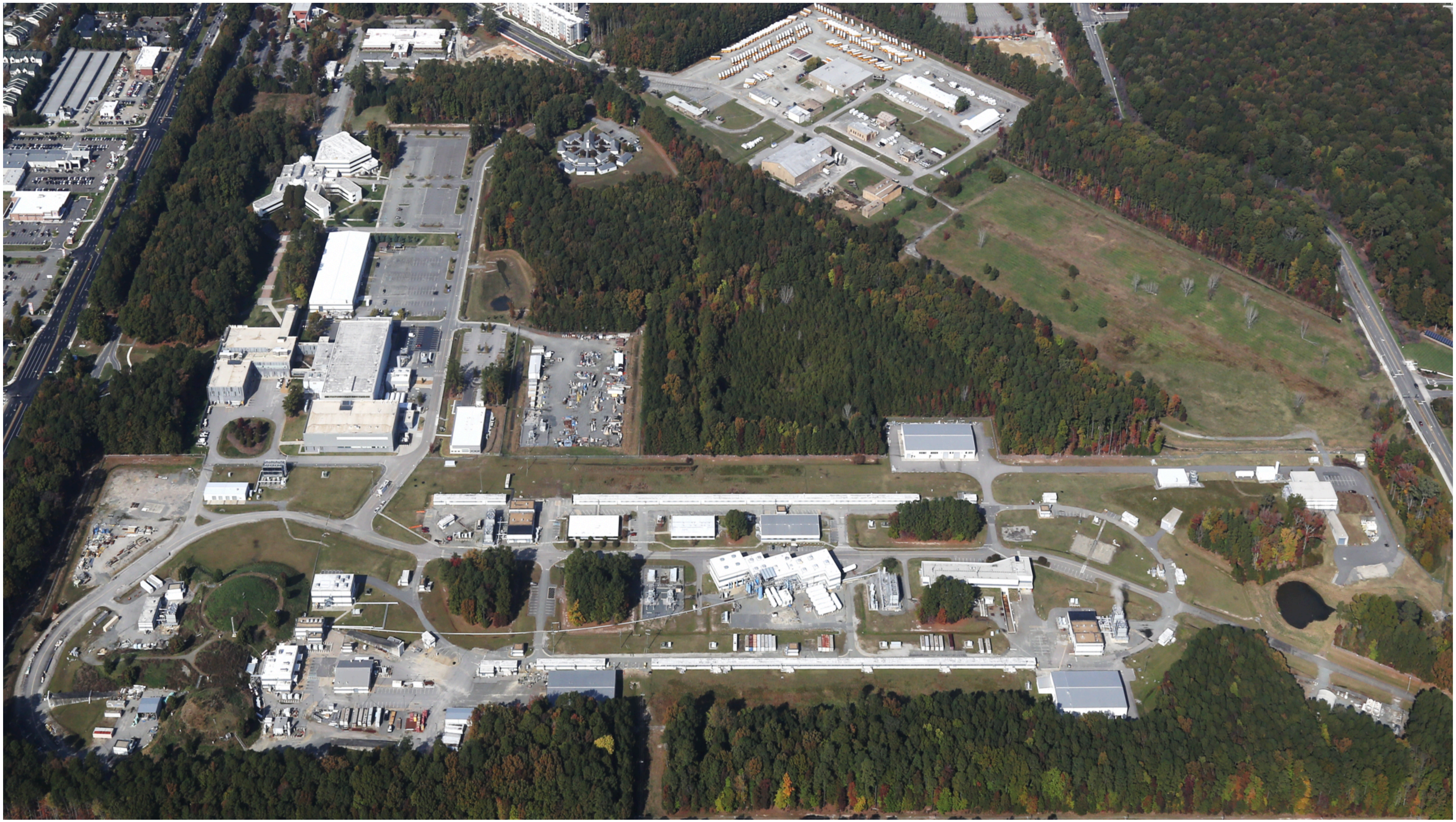

Continuous Electron Beam Accelerator Facility at Jefferson Lab

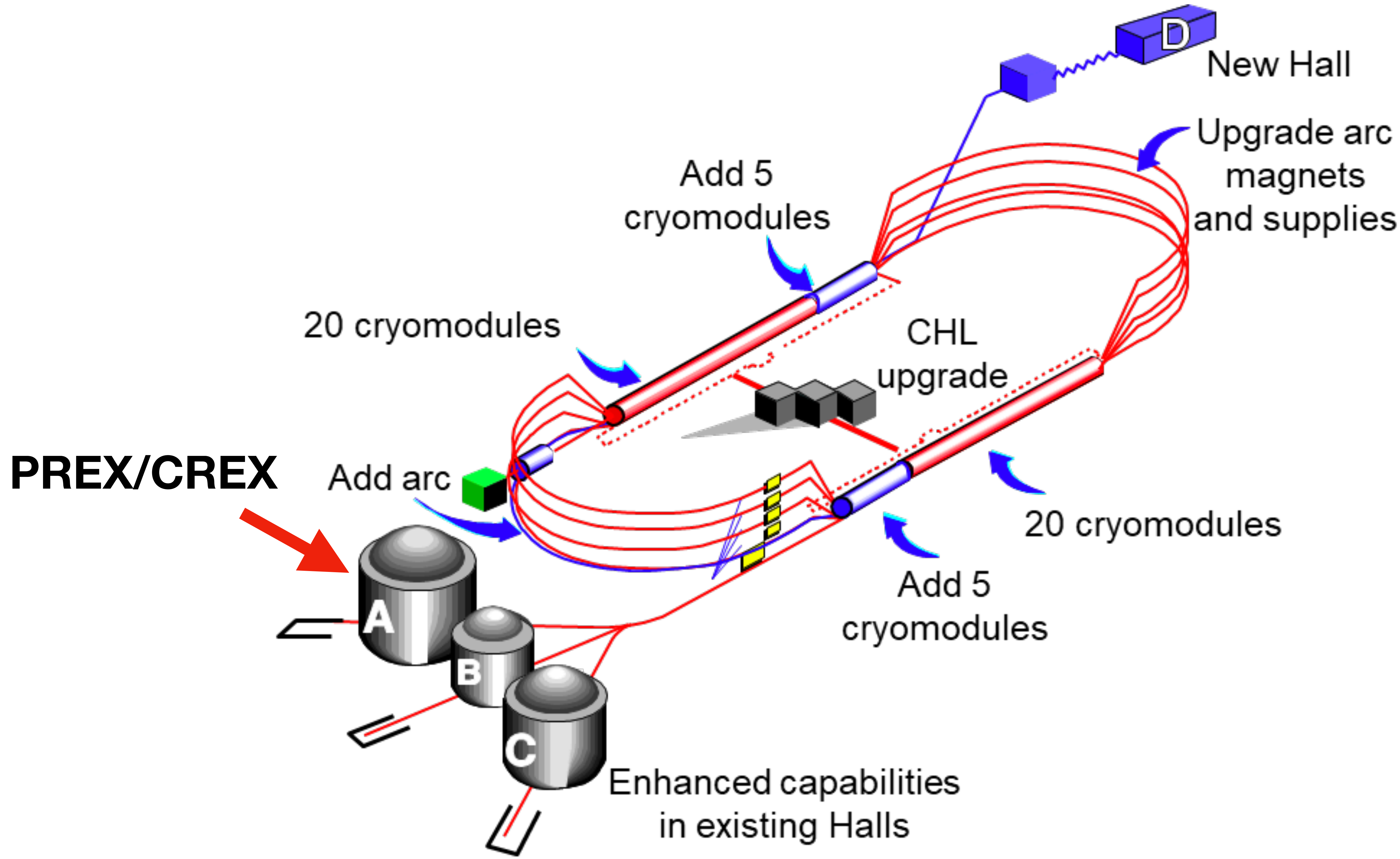

PVES at JLab

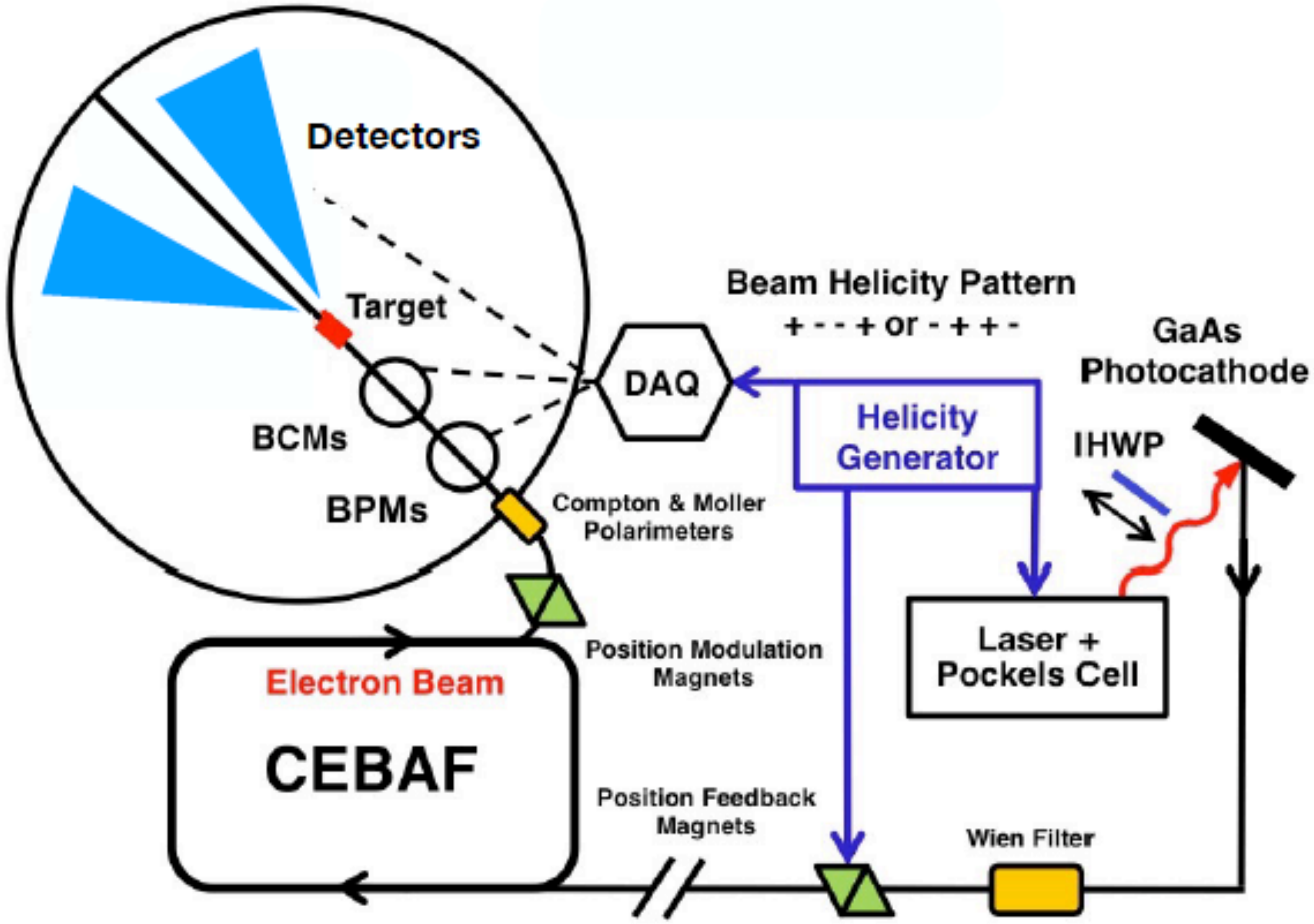

Detectors
Target
BCMs
BPMs
DAQ
Beam Helicity Pattern
+ - - + or - + + -
GaAs
Photocathode
Helicity
Generator
IHWP
Compton & Moller
Polarimeters
Laser +
Pockels Cell
Position Modulation
Magnets
Electron Beam
CEBAF
Position Feedback
Magnets
Wien Filter

PVES at JLab

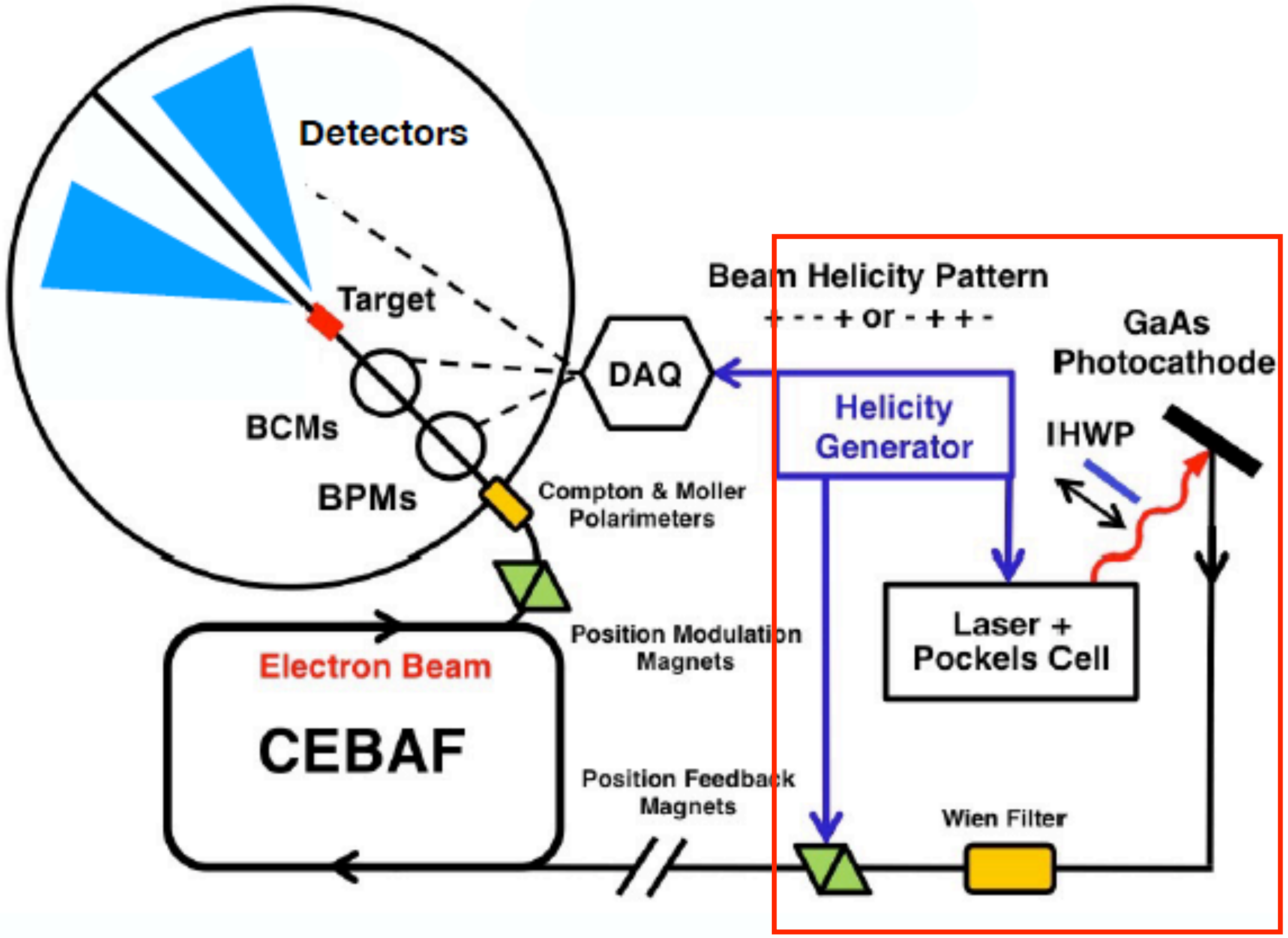

Injector:

- Up to 180 uA
- Polarization ~90%
- Up to 1kHz helicity flip

- Fast helicity flipping relies on **Pockels Cell**.
- Slow helicity flipping relies IHWP and Wien Filter

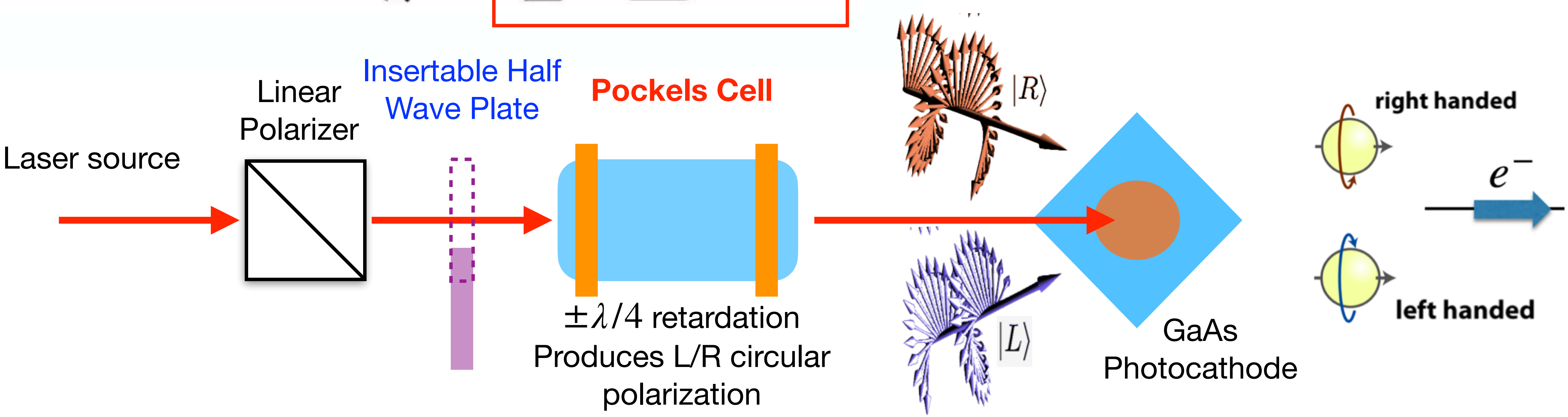

PVES at JLab

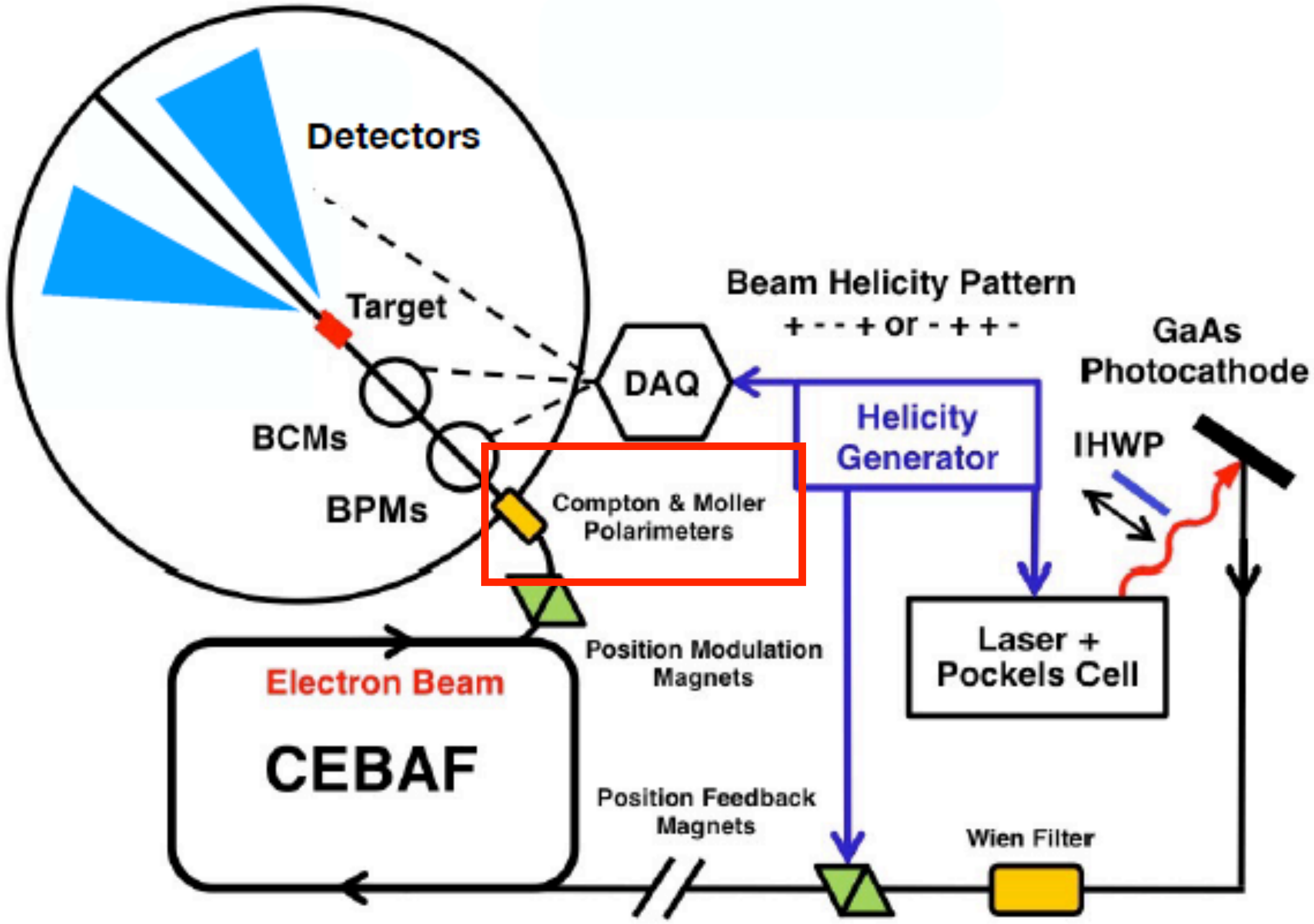

Polarimeters:
- Mott at Injector
- Compton and Moller at Hall
- ~1% level precision

Moller Polarimetry

- Polarized cross section asymmetry of Moller scattering (elastic electron-electron scattering)
- Rapid, high precision measurement; **Destructive** only low beam current

$$\sigma \sim 1 + \sum_{i=X,Y,Z} (A_{ii} \cdot P_i^{targ} \cdot P_i^{beam})$$

$$A_{ZZ} = -\frac{\sin^2\theta_{CM} \cdot (7+\cos^2\theta_{CM})}{(3+\cos^2\theta_{CM})^2}$$

Energy independent

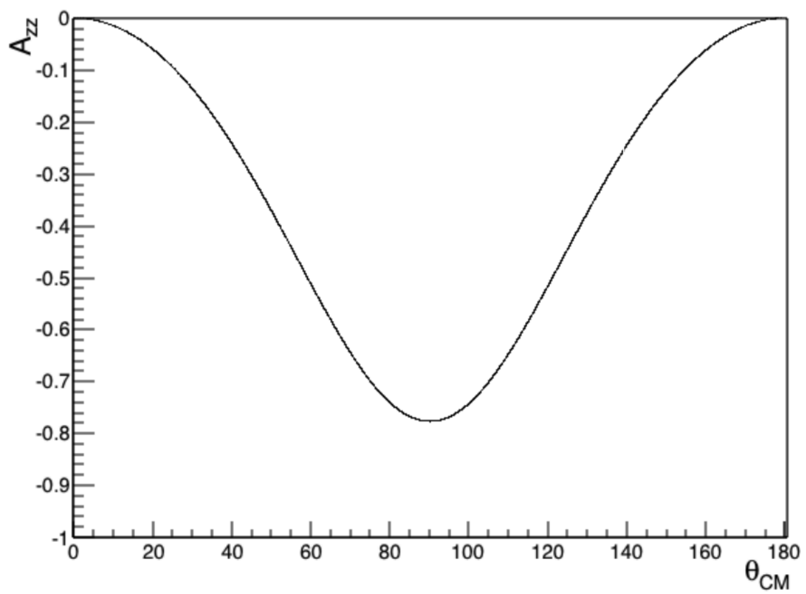

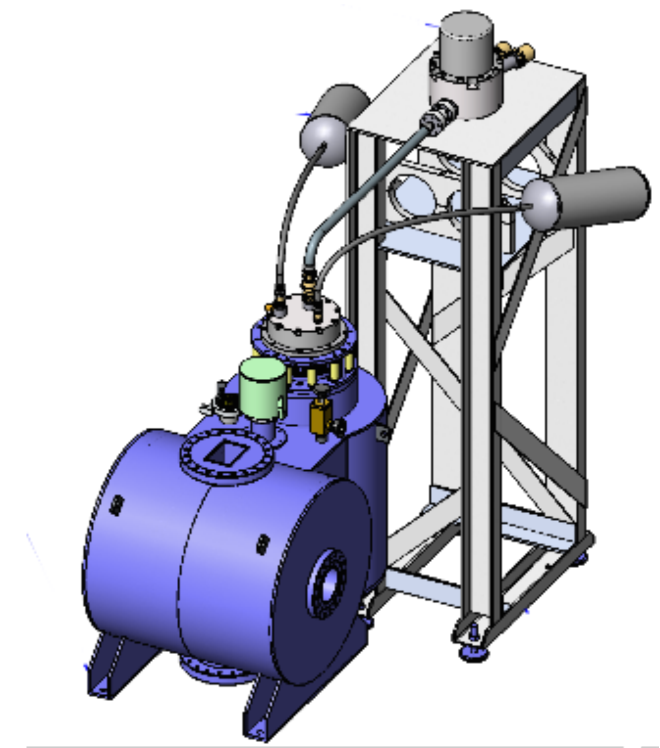

Iron Foil Target in high-field superconductor magnet.

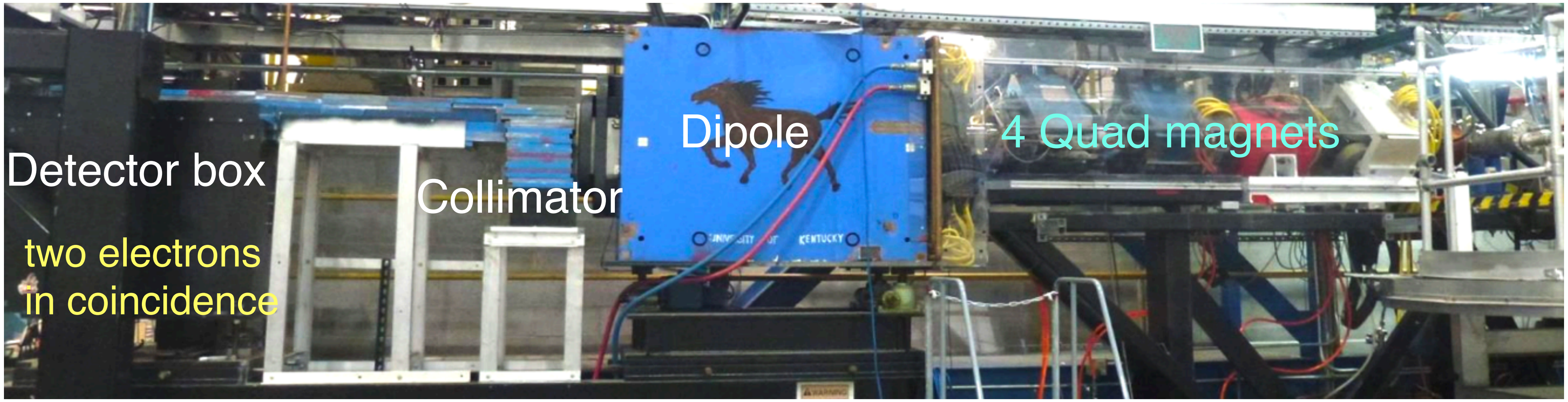

Compton Polarimeter

Polarized cross section asymmetry of Compton scattering

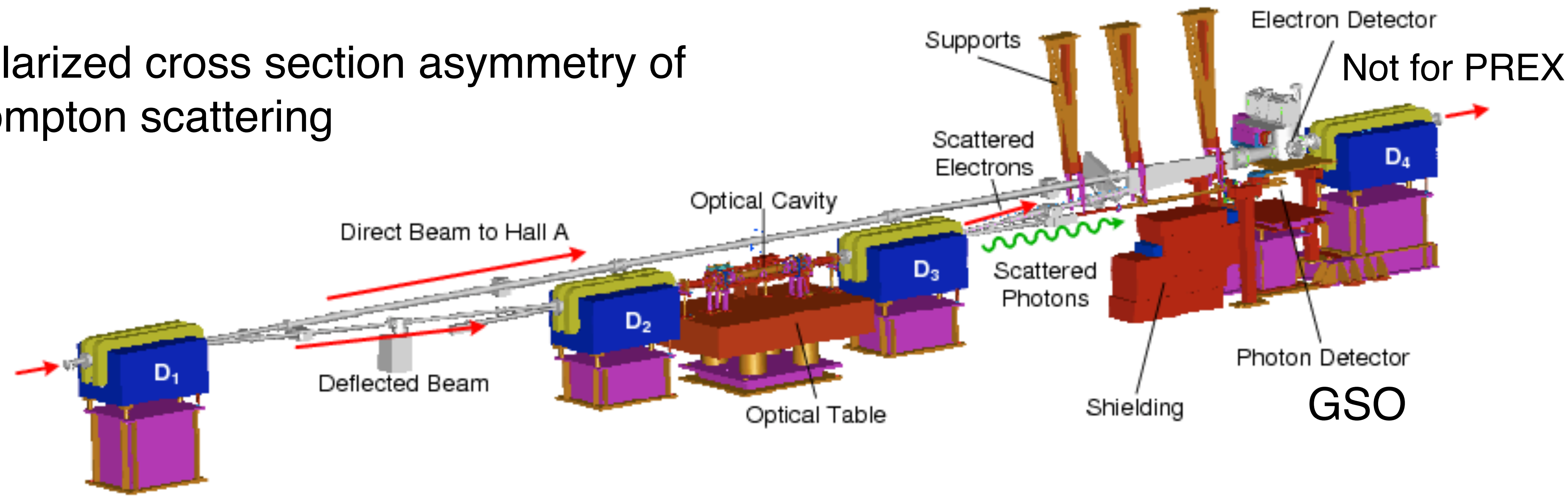

- 4-dipole chicane, **non-destructive** measurement: **continuous** monitoring of beam polarization
- Laser beam colliding with electron beam nearly head-on
- Integrating DAQ;
  GSO used to detect scattered photons;
  Diamond microstrips used to detect scattered electrons
- PREX2 will need 1% at 950 MeV
  CREX will need 0.8% at 2.22GeV

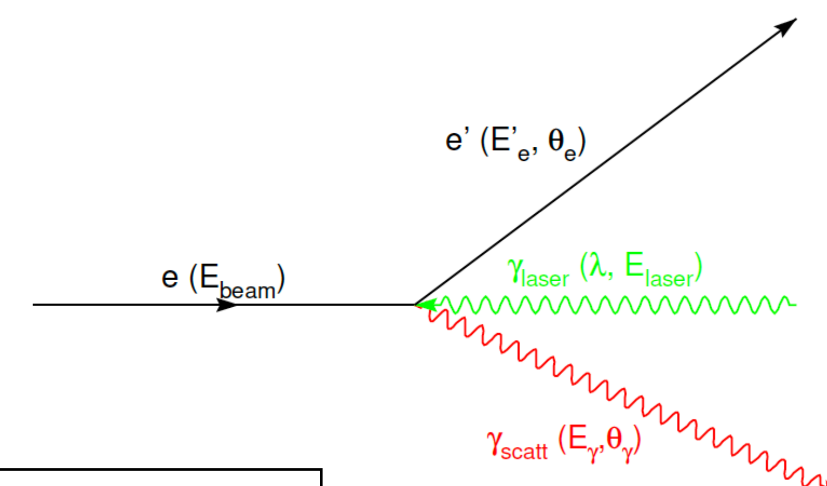

CREX Polarimetry Result:
Pe=87.09 +/- (0.44% dP/P)

PVES at JLab

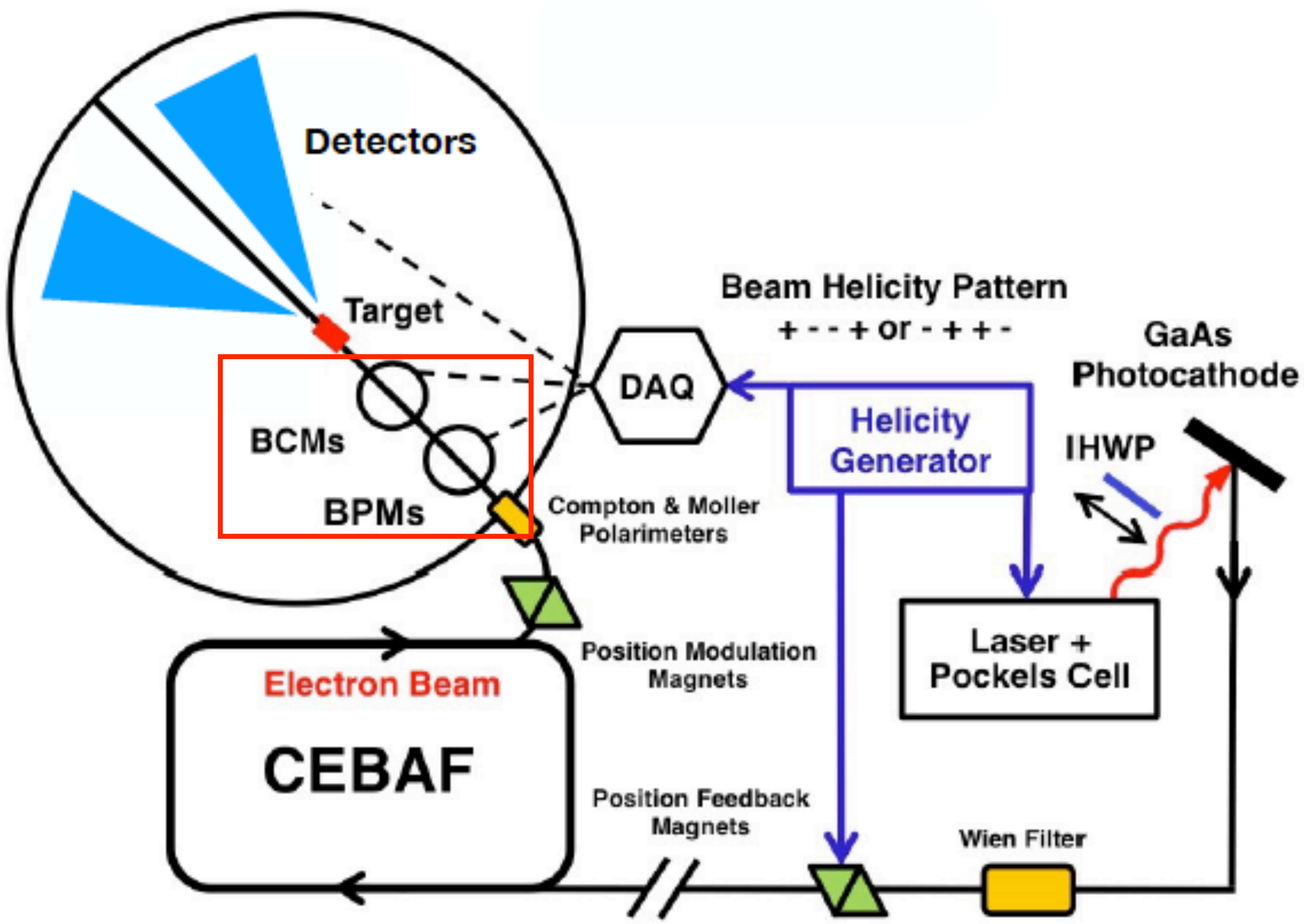

Beam monitoring:

- RF antenna or RF resonating cavities
- Charge ~30ppm, position ~1um
- Fast feed back to injector

Beam Monitoring

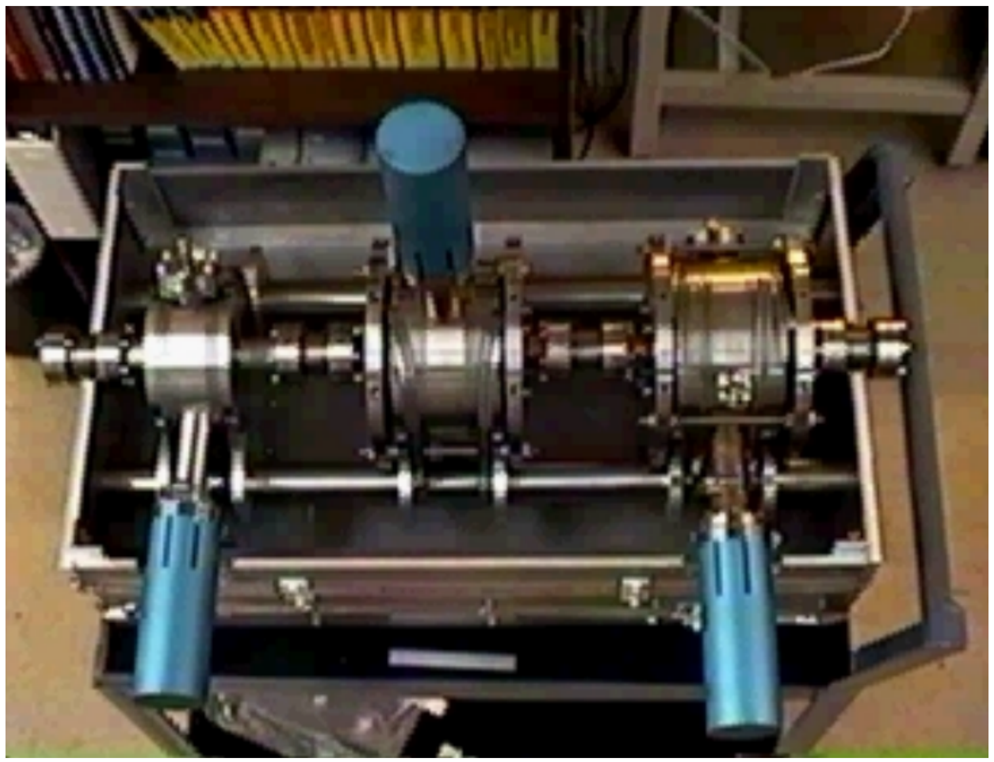

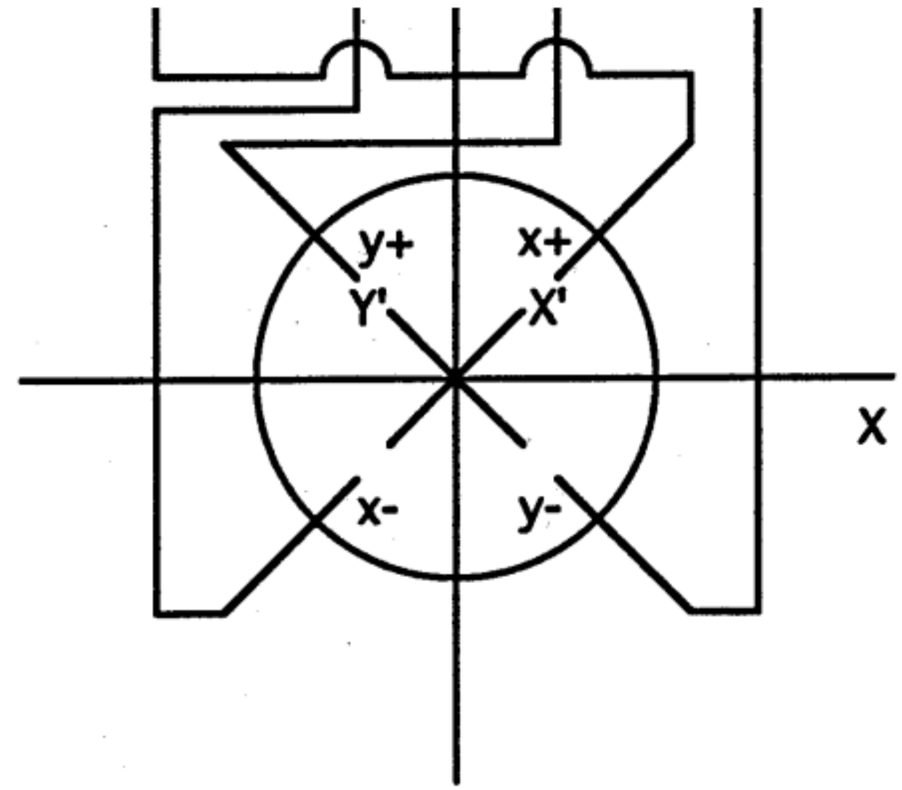

- Mostly use RF resonating cavities or RF antennas
  - can measure beam charge to about 30 ppm and positions to about 1 micron
- Electronics are used to **fast feedback** and reduce large helicity correlated beam asymmetries

PVES at JLab

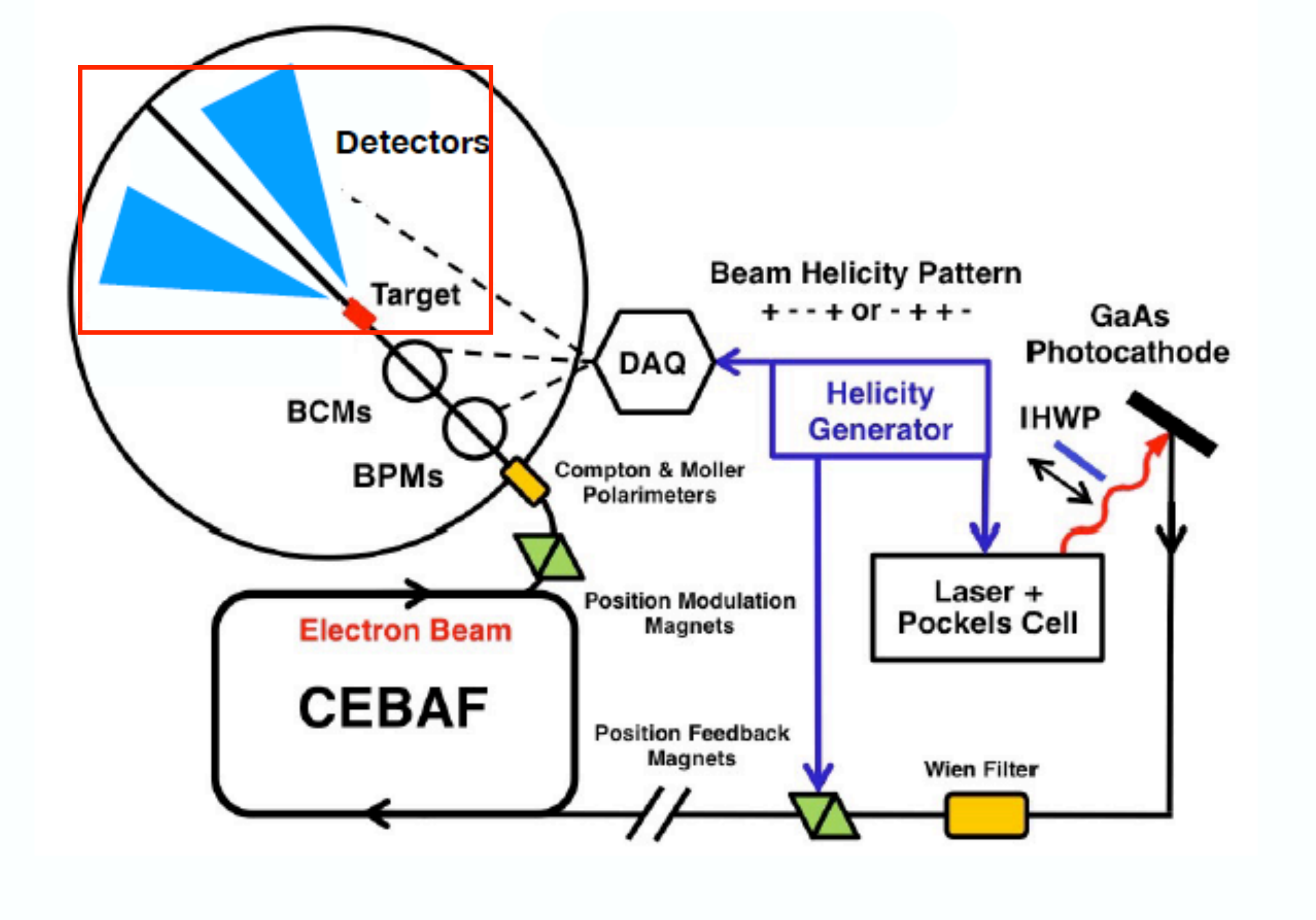

Spectometers:

- HRS - High Resolution Spectrometers
- dp/p ~ 2x10^{-4}

Hall A High Resolution Spectrometers

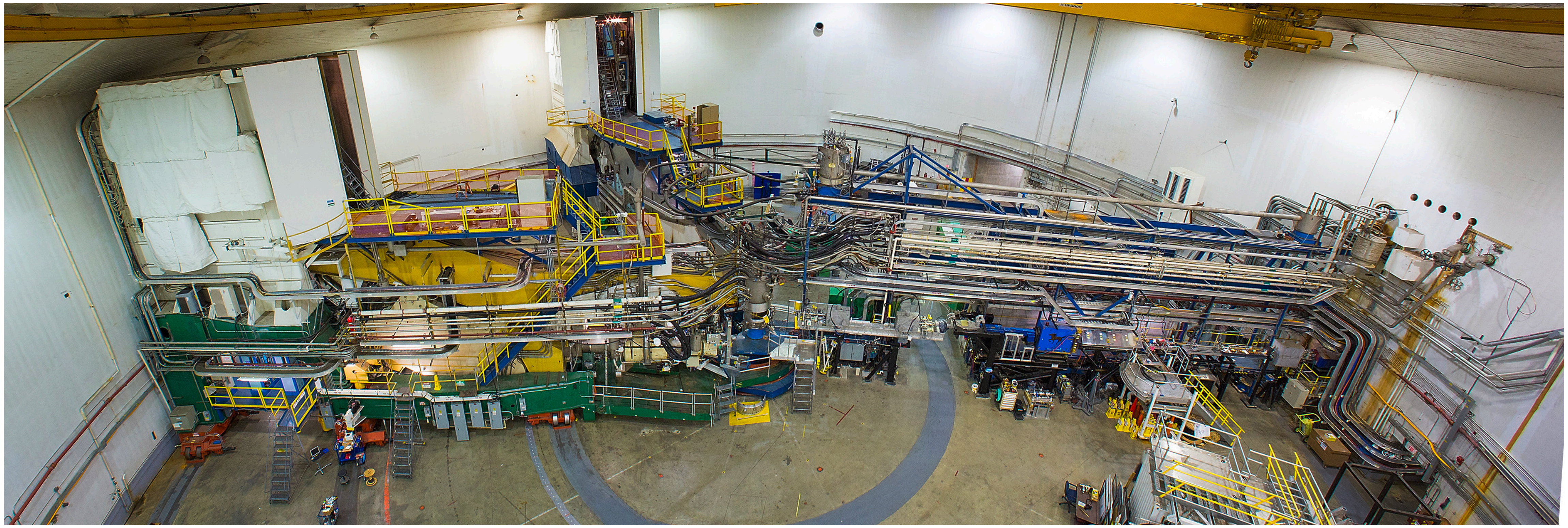

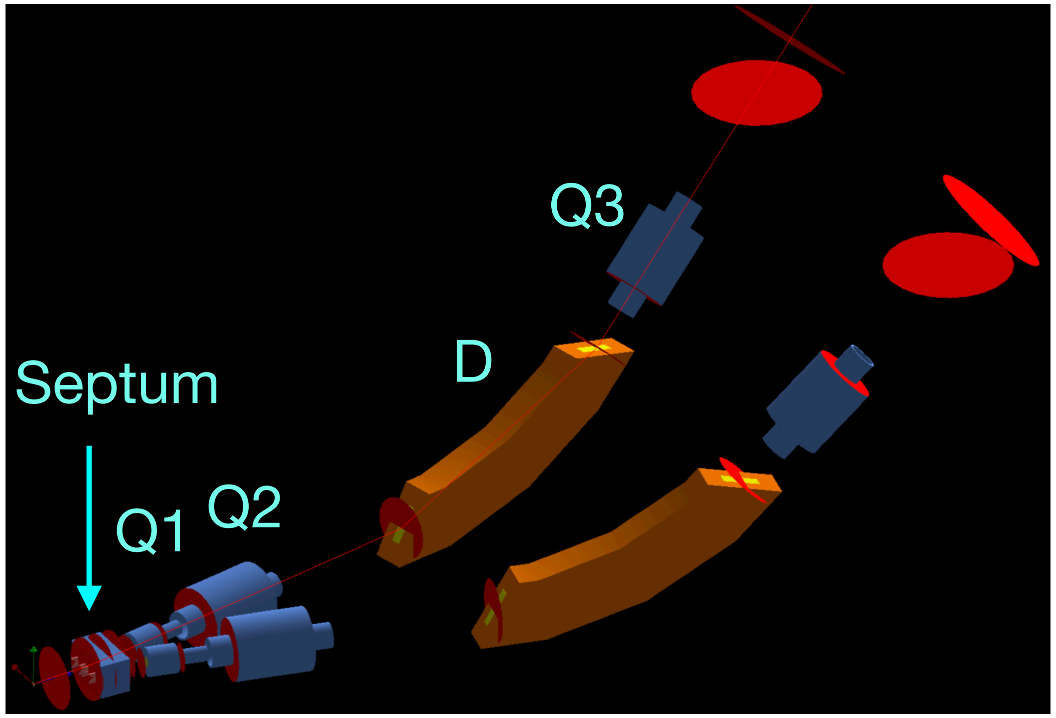

- Resolve elastic scattering
- Discriminate excited states
- dp/p ~ 2×10^{-4}

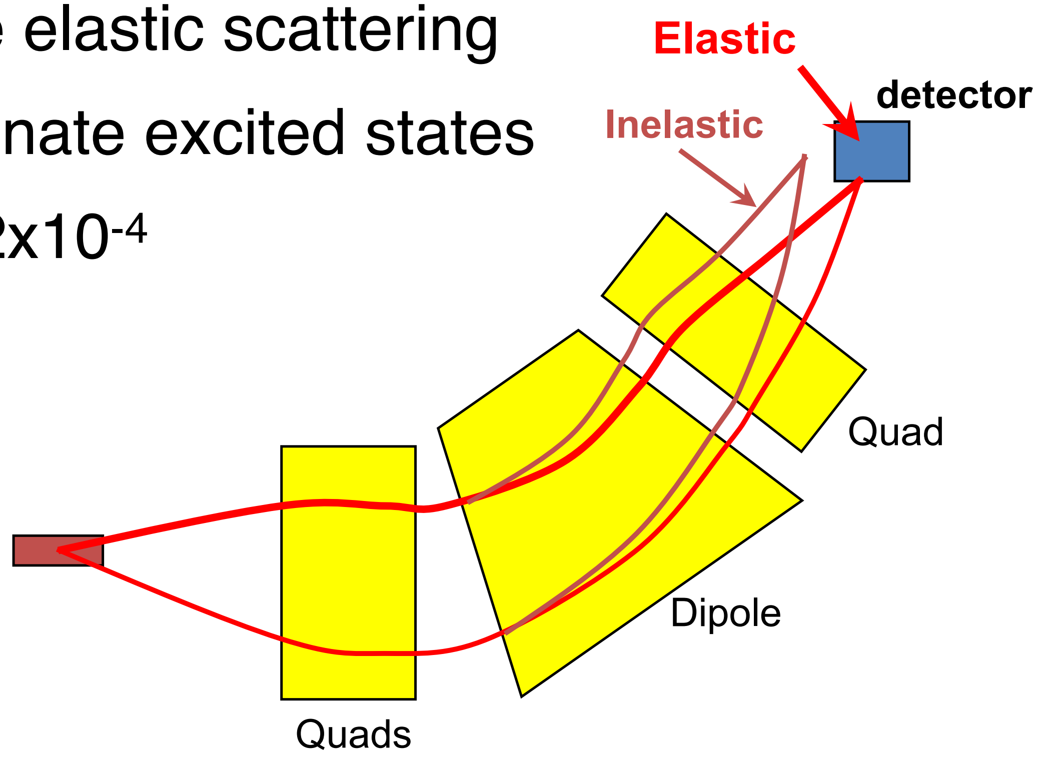

Main Detectors

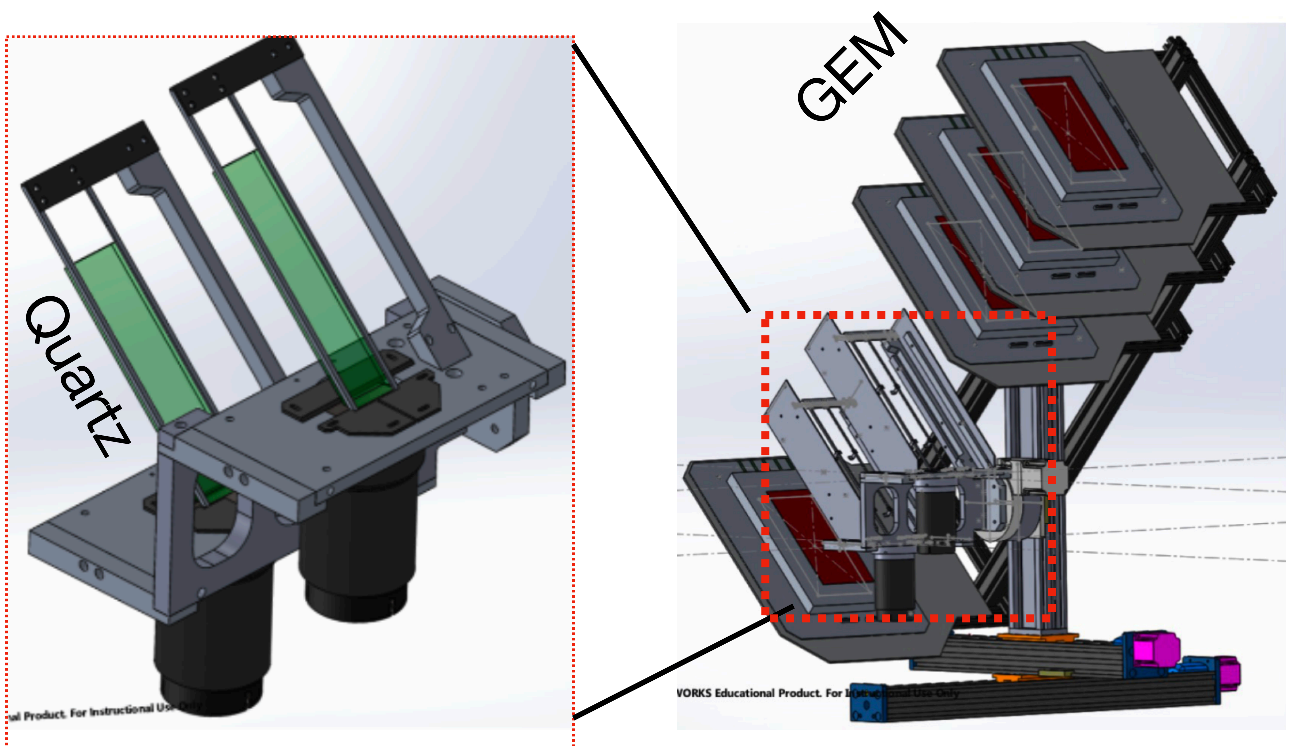

D. McNulty

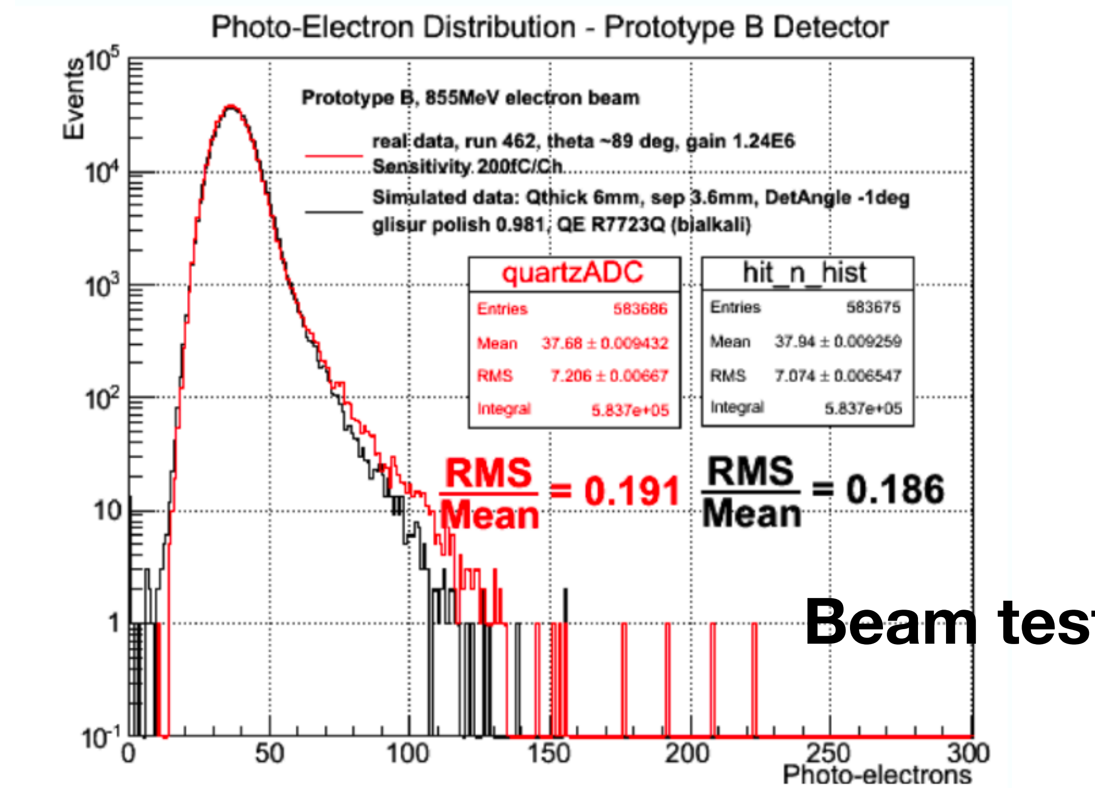

- Fused silica Cherenkov radiator, 5mm thick 3.5x16 cm2 area, mated to a single PMT
  - Non-linearity of detector response was tested on the bench and with beam during the experiment
- GEMs for tracking runs (Q^2 measurement)

Determining central scattering angle and Q^2

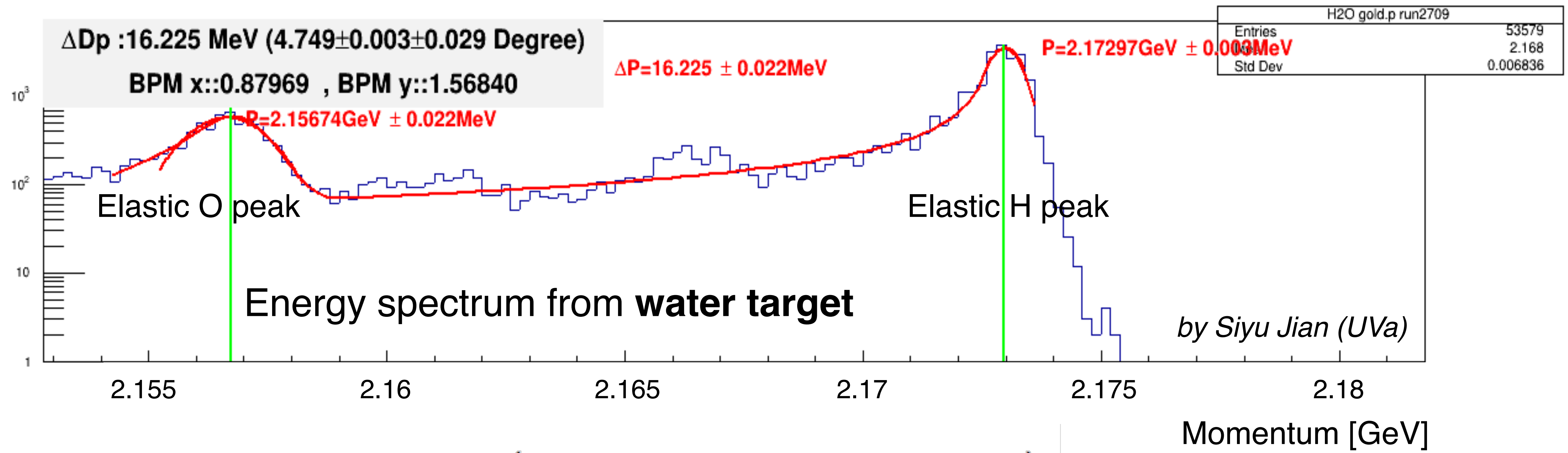

$$\Delta E' = E'_O - E'_H = E\left(\frac{1}{1+\frac{2E\sin^2(\frac{\theta}{2})}{M_O}} - \frac{1}{1+\frac{2E\sin^2(\frac{\theta}{2})}{M_H}}\right)$$

- ^{1}H and ^{16}O in one target (same E-loss) provides measurement of angle θ
- Nuclear recoil method recoil momentum difference ⟶ scattering angle
- Determined central angle with pointing with precision of $\delta\theta = 0.02^0$ (0.45%)

PREX <Q2> = 0.00616 ± 0.00004 GeV^2 (δ Q2/Q2 = 0.65%)

PREX/CREX Target

- Lead has low melting point, and low thermal conductivity
- Diamond foils have excellent thermal conductivity, Helium cooled
- ^{12}C is isoscaler, spin-0 (and well-measured) harmless background

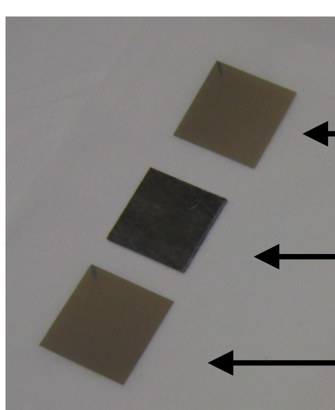

Diamond

Lead

Diamond

Cryogenic production target ladder

- ~5.7 mm thick
- ~91.7% ^{48}Ca, ~7.96% ^{40}Ca

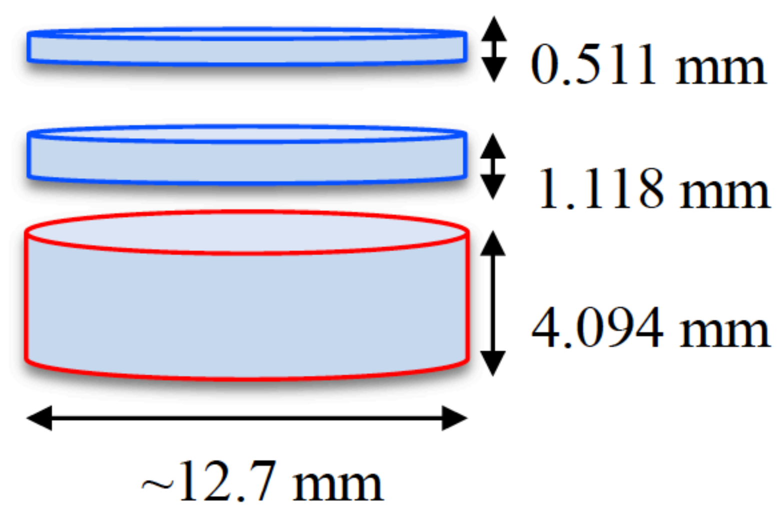

Scattering Chamber

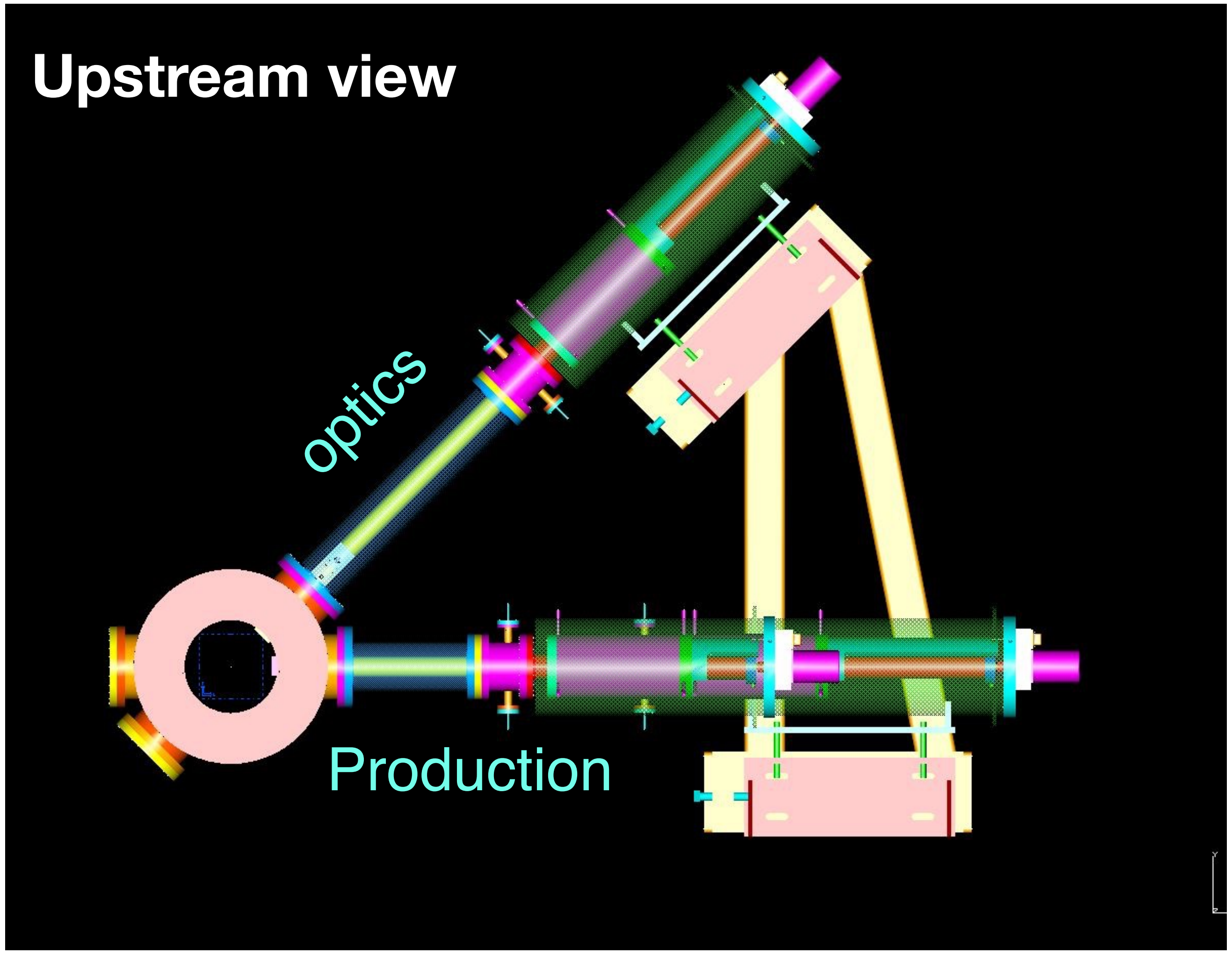

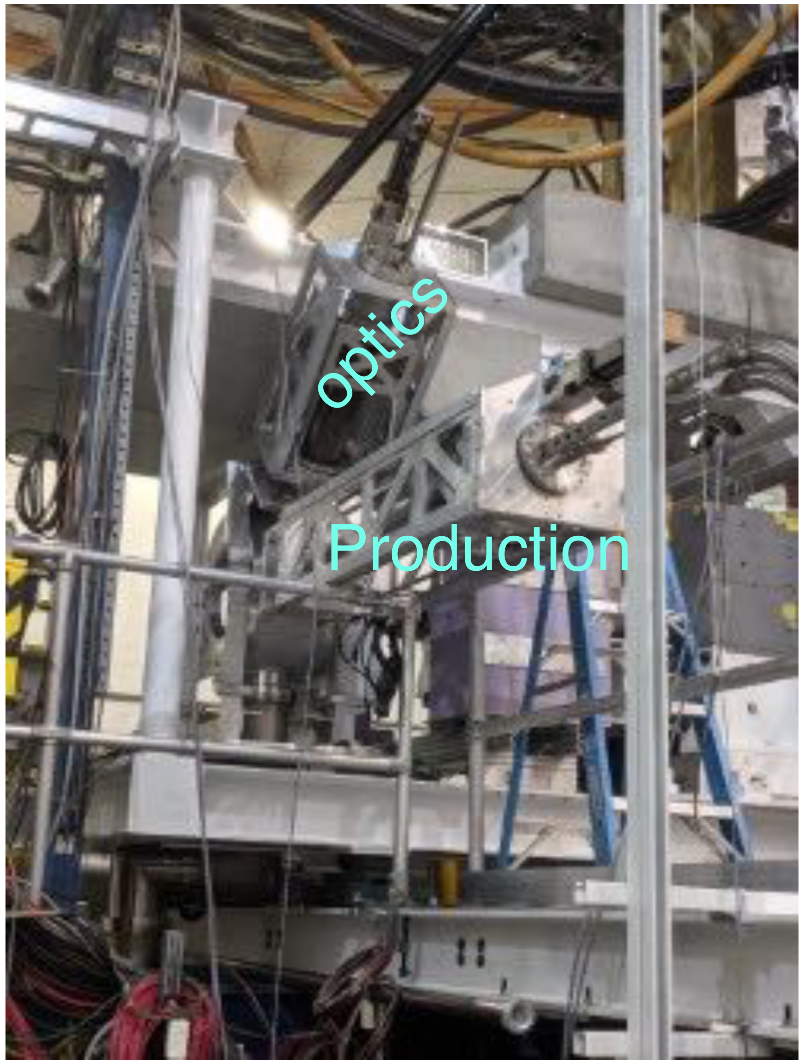

- One cryogenic production target ladder and one optics ladder at single target location
- Improved based on lessons learned during PREX-I
- Solves vacuum and mechanical assembly considerations

Radiation Shielding

PREX-I distributed significant power in the hall, damaging vacuum and electronics

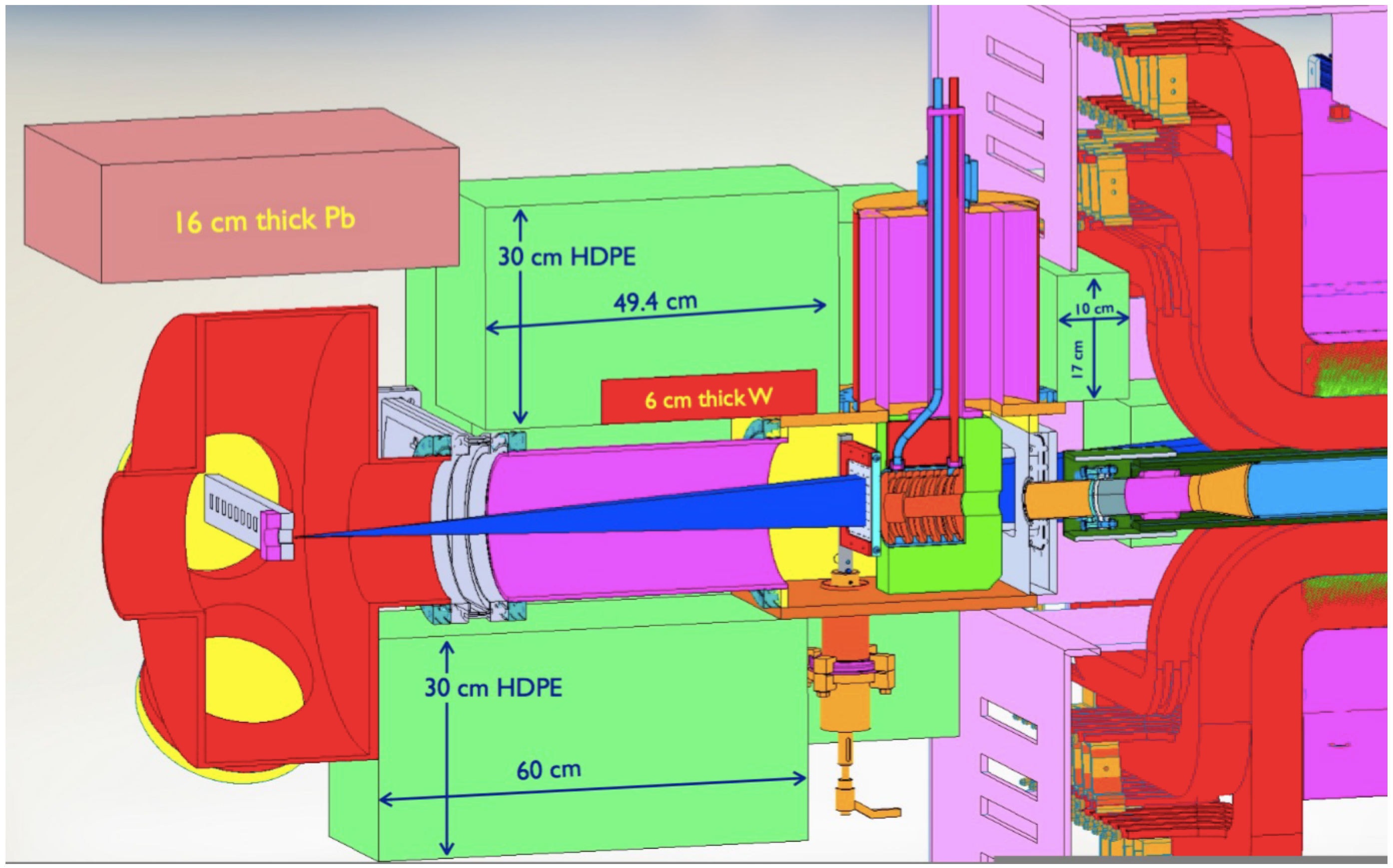

	PREX-I	PREX-II	CREX
Power in collimator (W/µA)	9.7	**28.8**	6.8
Power in hall (W/µA)	18.0	**3.0**	~1.5

Solution: Localize power in hall at collimator, and shield it

- Heavy concrete shielding over the target and collimator region to reduce the boundary dose
- Collimation and shielding protect sensitive electronics inside the hall

Integrating DAQ

Flux integration Technique

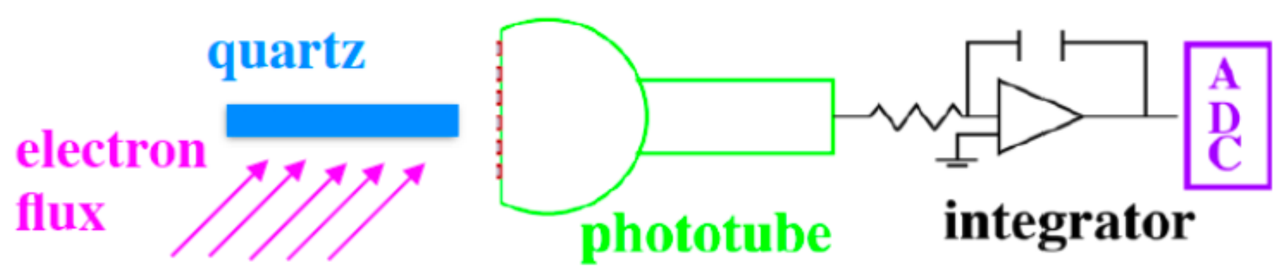

CREX rate: 500 MHz
PREX rate: 2GHz

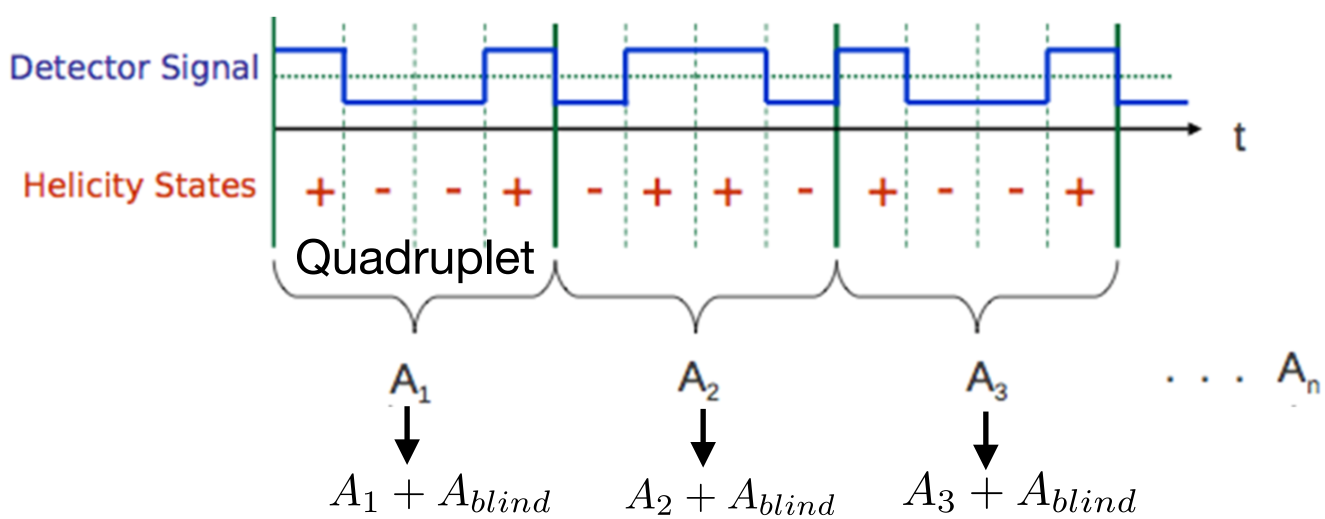

$$A_i = sign_1 \times \frac{D_1/I_1 - D_2/I_2 - D_3/I_3 + D_4/I_4}{D_1/I_1 + D_2/I_2 + D_3/I_3 + D_4/I_4}$$

D: detector signal, I: beam current

Continuous Wave (CW) laser which flips helicity fast enough to make sure that experimental conditions do not change from one helicity signal to the other

Integrating, not counting (total number of detected electrons was ~6e+15

dominated by counting statistics fairly

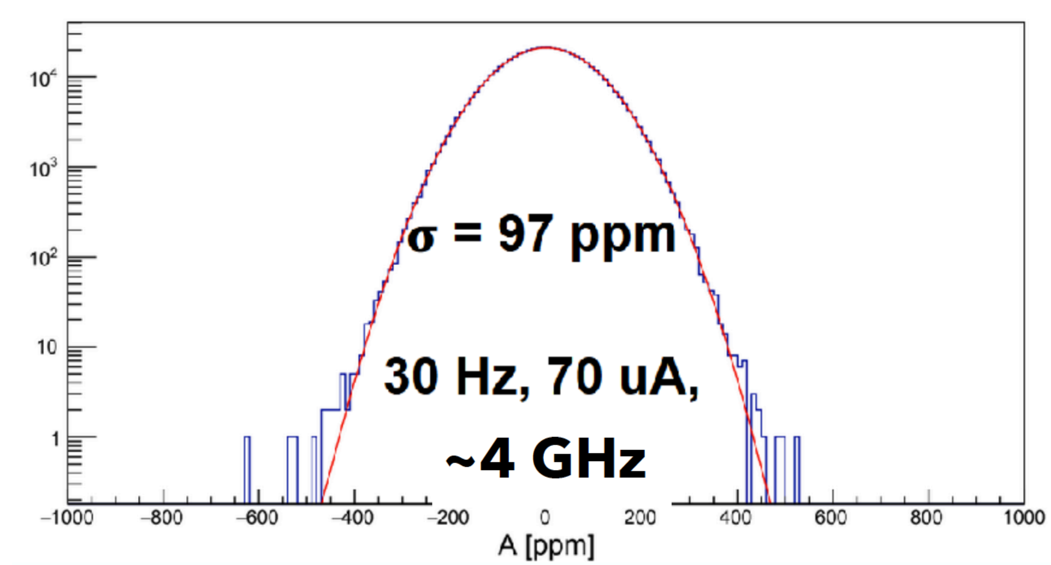

Time Line

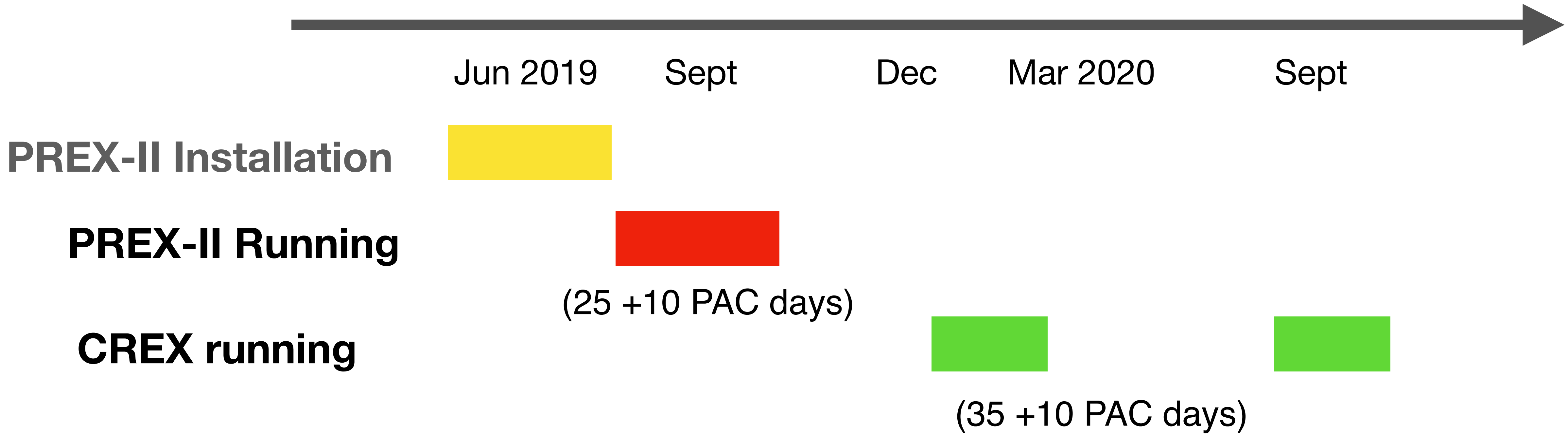

Jun 2019
Sept
Dec
Mar 2020
Sept
PREX-II Installation
PREX-II Running
(25 +10 PAC days)
CREX running
(35 +10 PAC days)

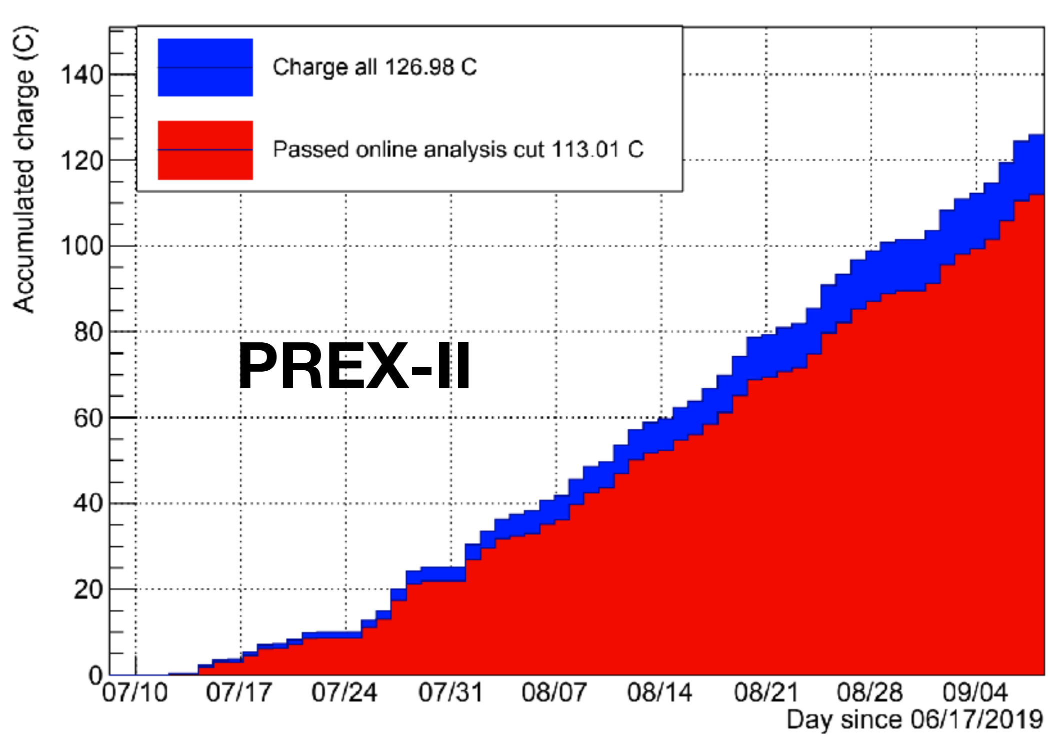

Accumulated charge (C)
Charge all 126.98 C
Passed online analysis cut 113.01 C
PREX-II
0
20
40
60
80
100
120
140
07/10
07/17
07/24
07/31
08/07
08/14
08/21
08/28
09/04
Day since 06/17/2019

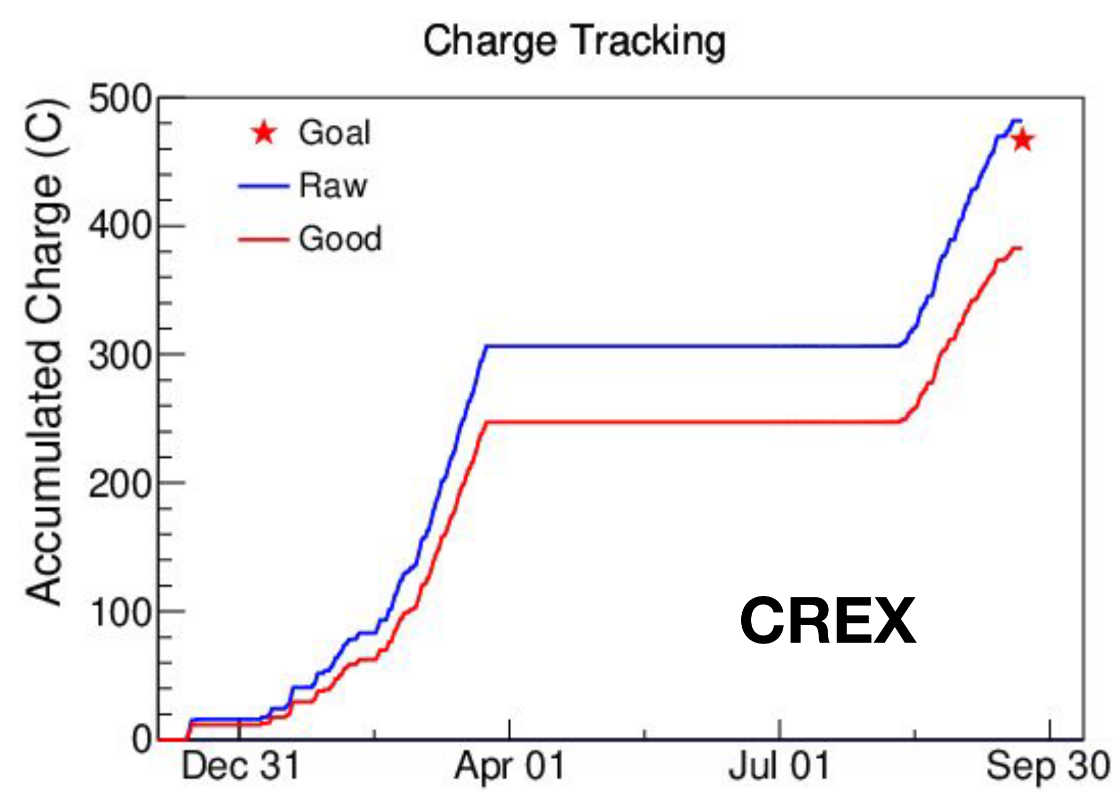

Charge Tracking
Accumulated Charge (C)
Goal
Raw
Good
CREX
0
100
200
300
400
500
Dec 31
Apr 01
Jul 01
Sep 30

PREX-II Data Overview

Corrected asymmetry

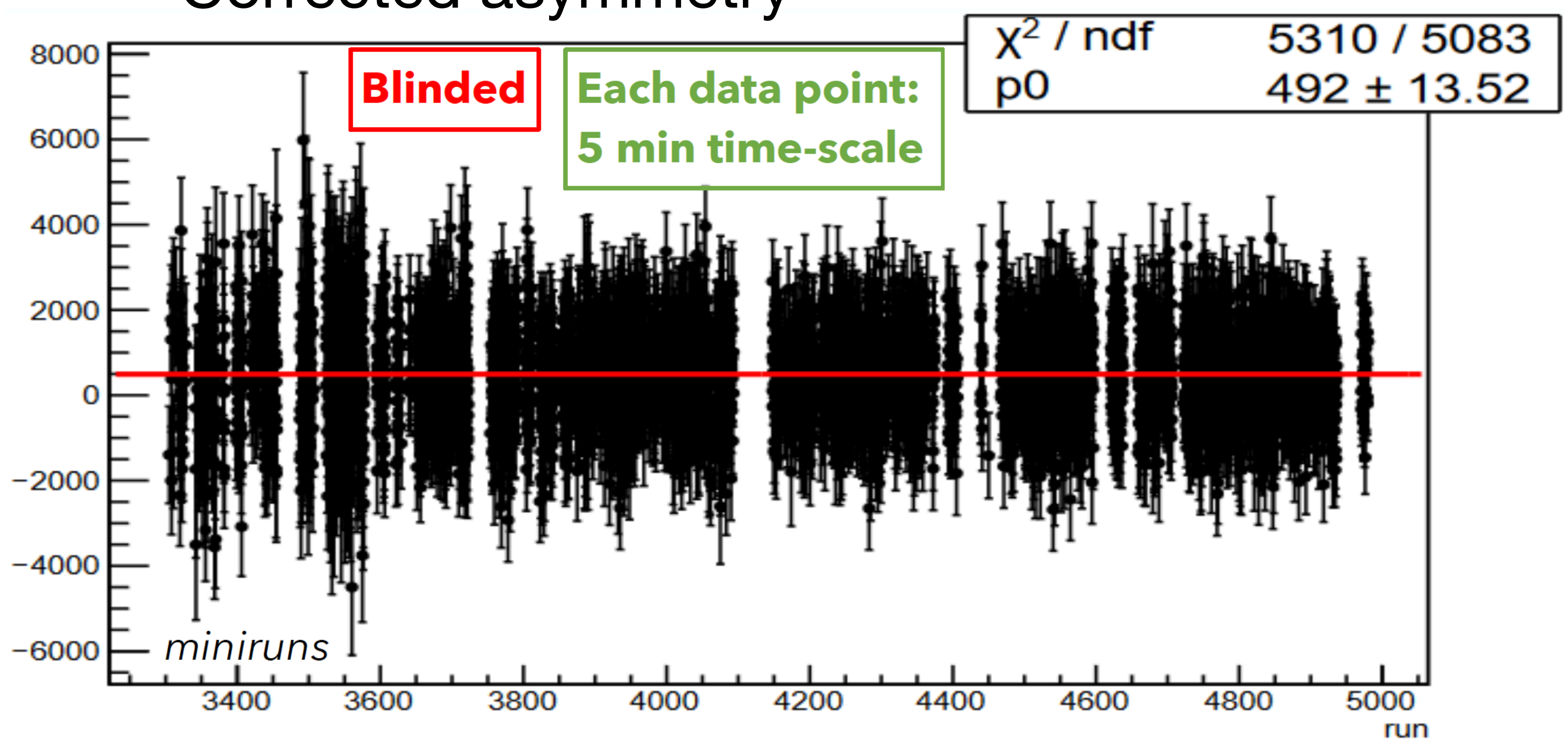

σ=0.995 ± 0.010

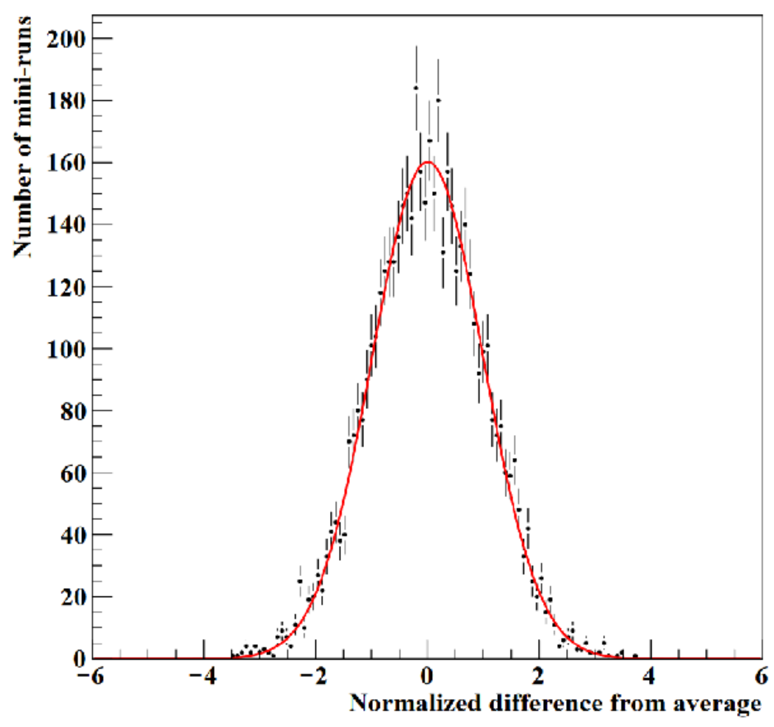

The corrected asymmetry removed effects from beam asymmetries and noise

“Blinding box”: an additive term on every octet asymmetry, randomly selected (flat) at the start of the run, from ± 160 ppb

PREX-II Data Overview

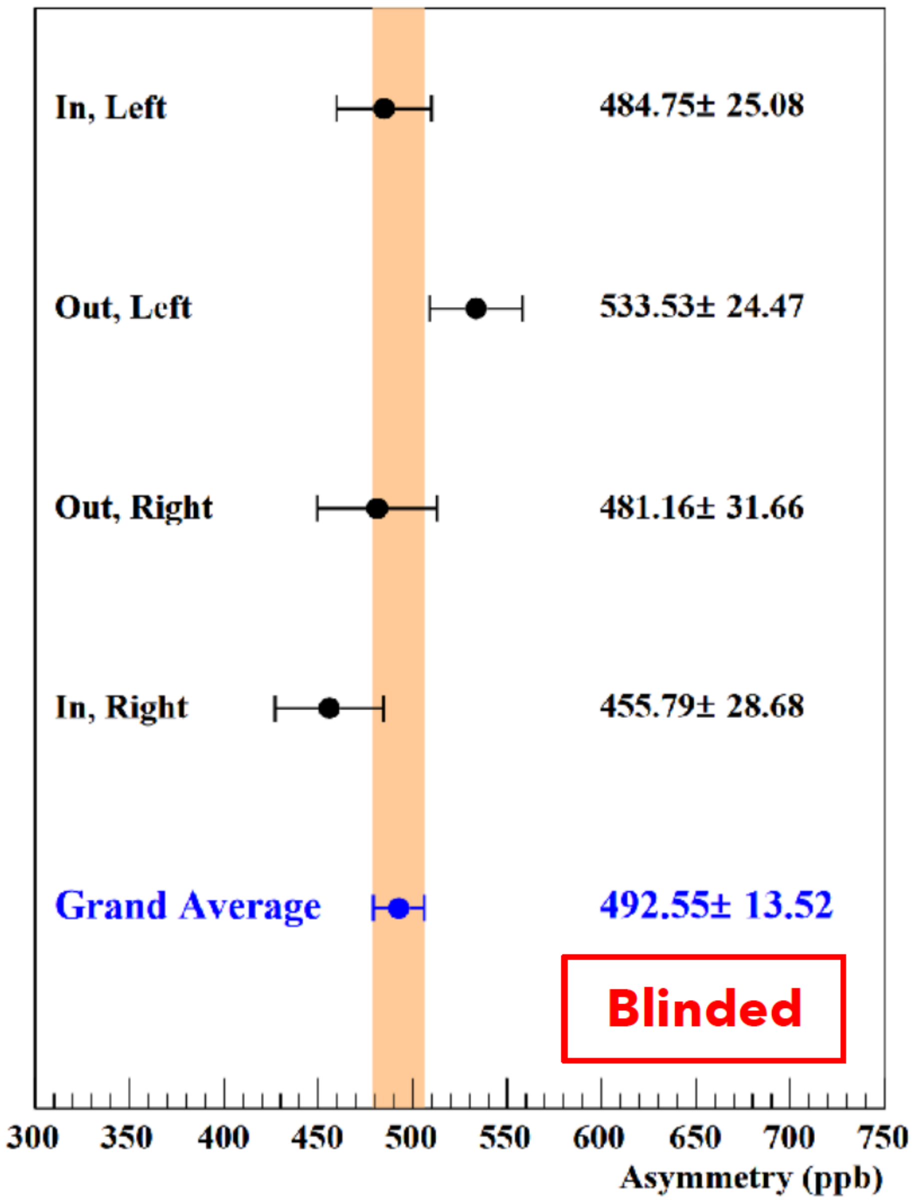

$$A_{PV} = R_{acceptNorm} \frac{A_{corr}/P_e - \sum_i A_i f_i}{1 - \sum_i f_i}$$

$$A_{corr} = A_{raw} + A_{beam} + A_{nonLin} - A_{blind}$$

	A_{PV} uncertainty contribution [ppb]	A_{PV} uncertainty contribution [%]
Polarization	5.23	0.95%
Acceptance normalization	4.56	0.83%
Beam correction	2.98	0.54%
Non-linear detector response	2.69	0.49%
Carbon dilution	1.45	0.26%
Charge correction	0.25	0.04%
Inelastic contamination	0.12	0.02%
Total	**8.16**	**1.48%**

When taken all into account the experimental systematic uncertainty comes to just ~1.5% (2% in proposal)

Unblinded A_{PV}: (550.0 ± 16.1)ppb

PREX-II Result

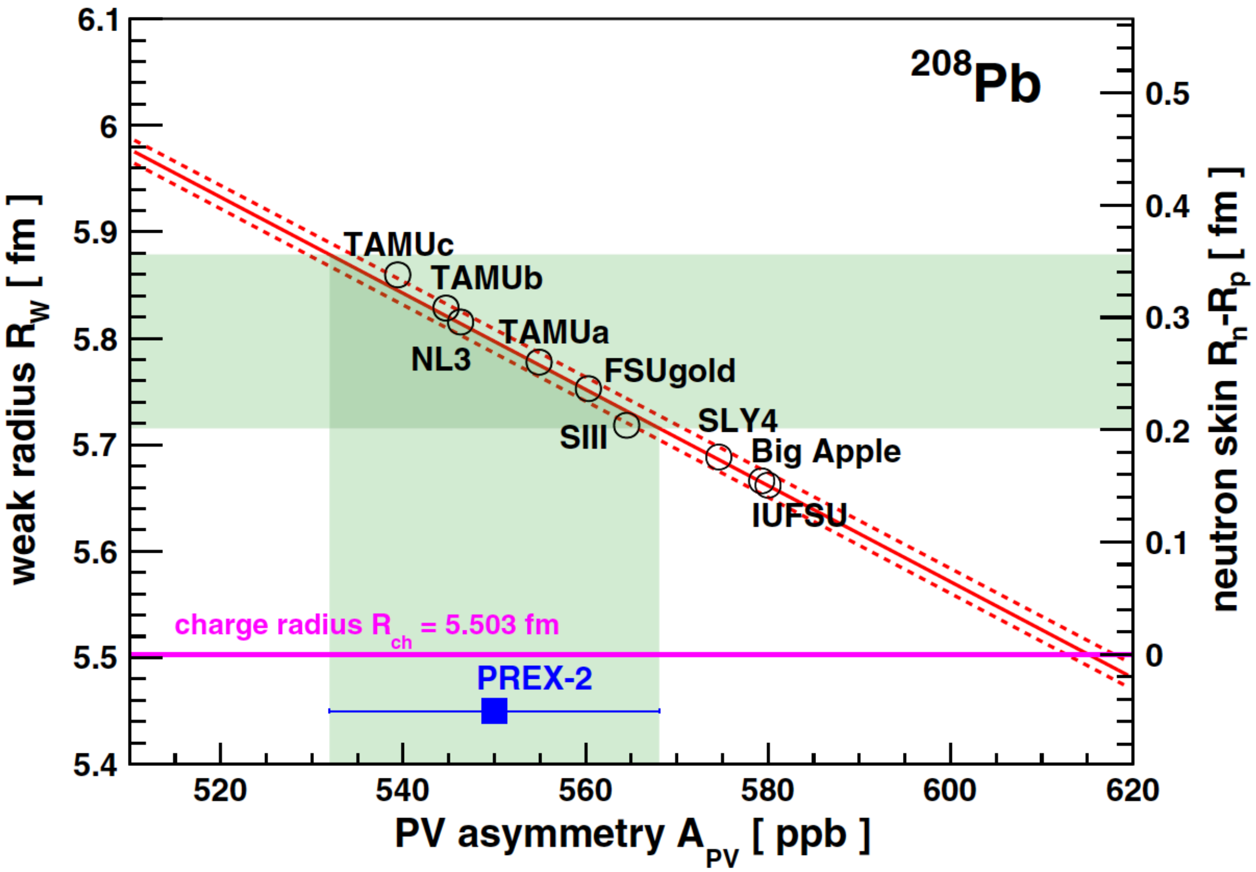

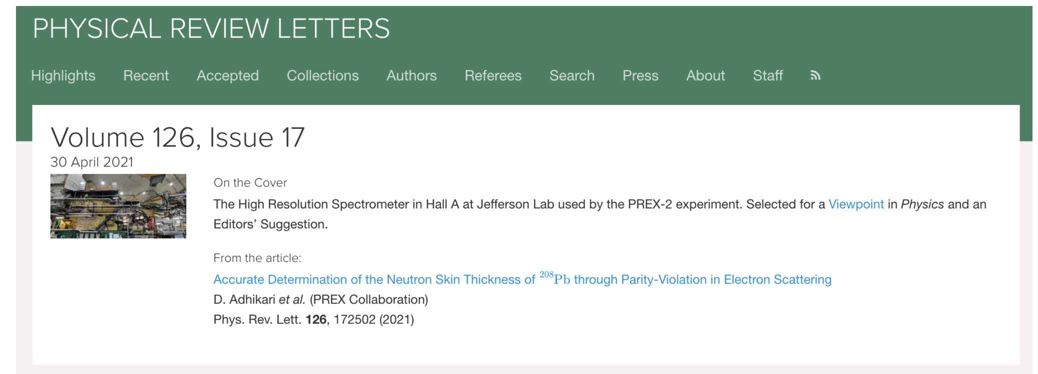

$$A_{\rm PV}^{\rm meas} = 550 \pm 16\,({\rm stat}) \pm 8\,({\rm syst})\ \ {\rm ppb}$$

$$F_W(\langle Q^2\rangle) = 0.368 \pm 0.013\,({\rm exp}) \pm 0.001\,({\rm theo})$$

$$R_W = 5.795 \pm 0.082({\rm exp}) \pm 0.013({\rm theo})\ \ {\rm fm}$$

$$R_n - R_p = 0.278 \pm 0.078({\rm exp}) \pm 0.012({\rm theo})\ \ {\rm fm.}$$

Combined PREX-I and PREX-II

^{208}Pb Parameter	Value
Weak radius (R_W)	5.800 ± 0.075 fm
Interior weak density (ρ_W^0)	-0.0796 ± 0.0038 fm^{-3}
Interior baryon density (ρ_b^0)	0.1480 ± 0.0038 fm^{-3}
Neutron skin ($R_n - R_p$)	0.283 ± 0.071 fm

- Consistent with PREX-I
- Did better than originally proposed statistical (±3%) and systematic (±2%) uncertainty goals

Impact on symmetry energy slope

Reed, Horowitz et al. PRL 126, 172503 (2021)

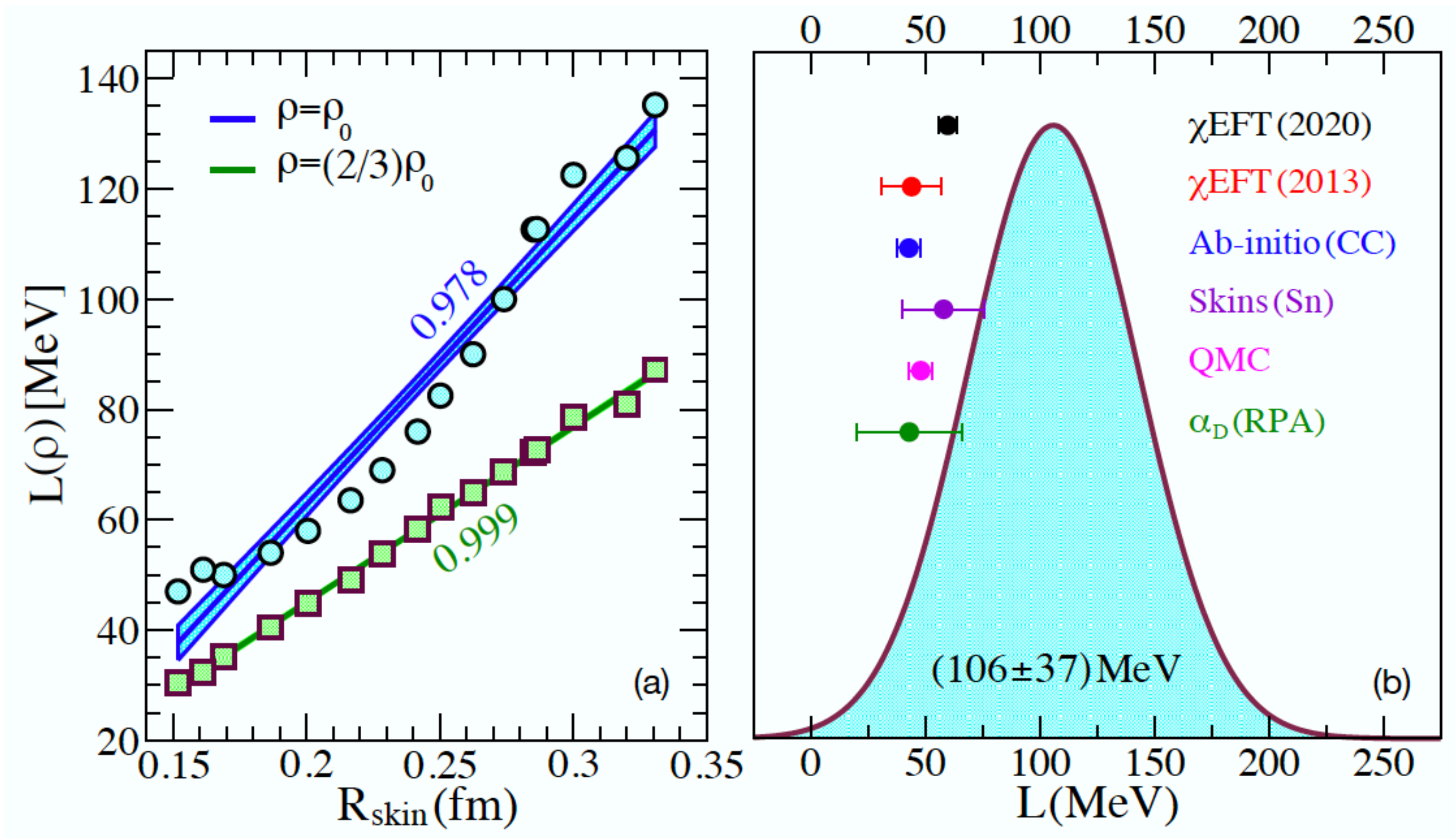

PREX result indicating a larger L (stiff EOS)

Implication on Neutron Star

Reed, Horowitz et al. PRL 126, 172503 (2021)

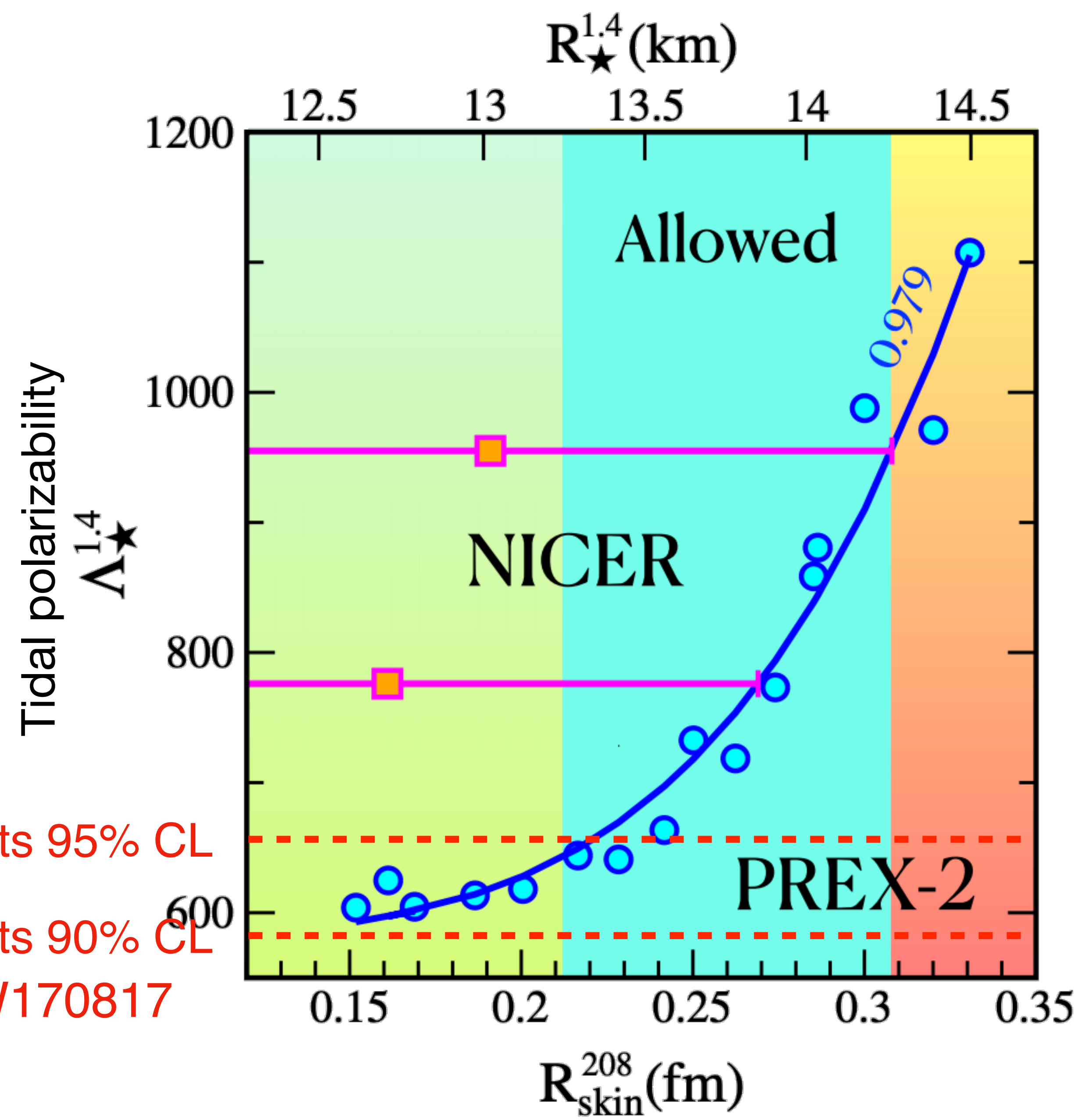

upper limits 95% CL

upper limits 90% CL
LIGO GW170817

- NICER (NASA's neutron star Interior Composition ExporeR) is an X-ray telescope on the International Space Station
- LIGO GW170817 provided upper limits for tidal polarizability < 580 neutron star radius and accordingly for neutron skin as well.
- Consistent with NICER, but tension with LIGO

Press attention

APS Viewpoint “highlighting exceptional research”

CREX Result

Sign-uncorrected, Each point: 8h time-scale

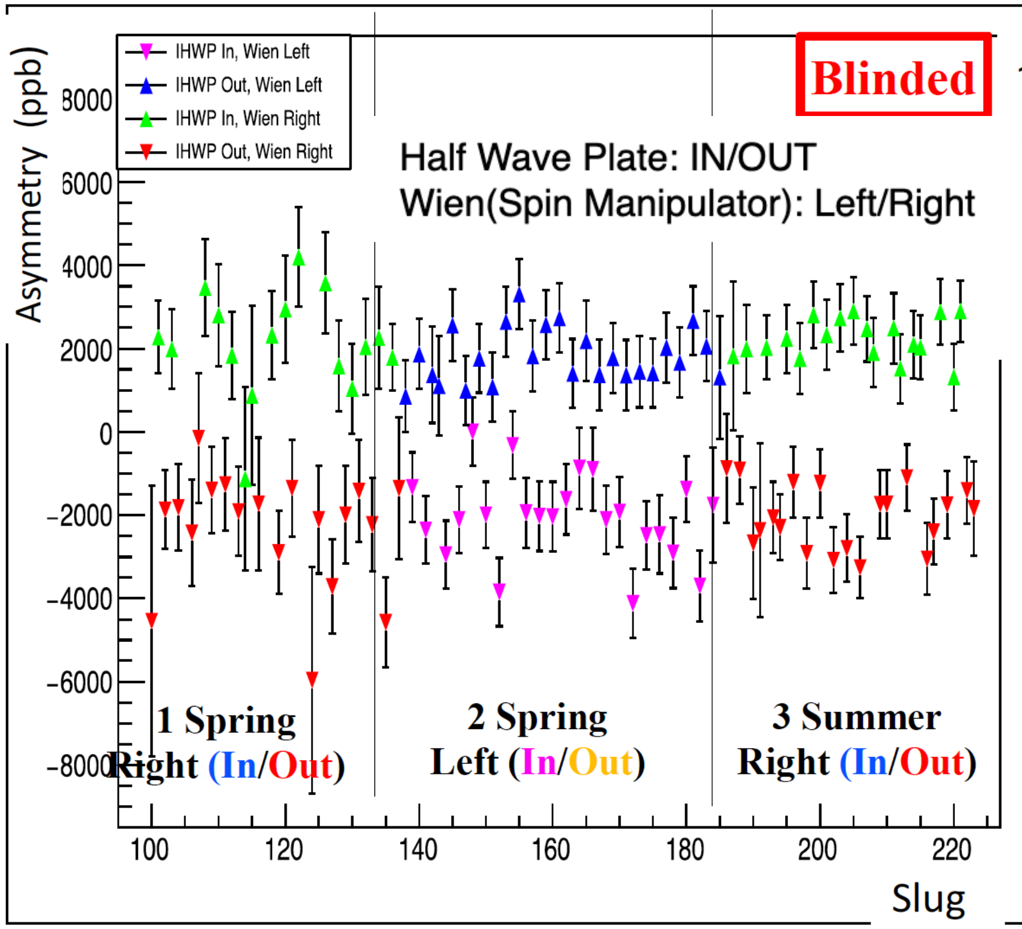

Sign-corrected, Each point: ~1week time-scale

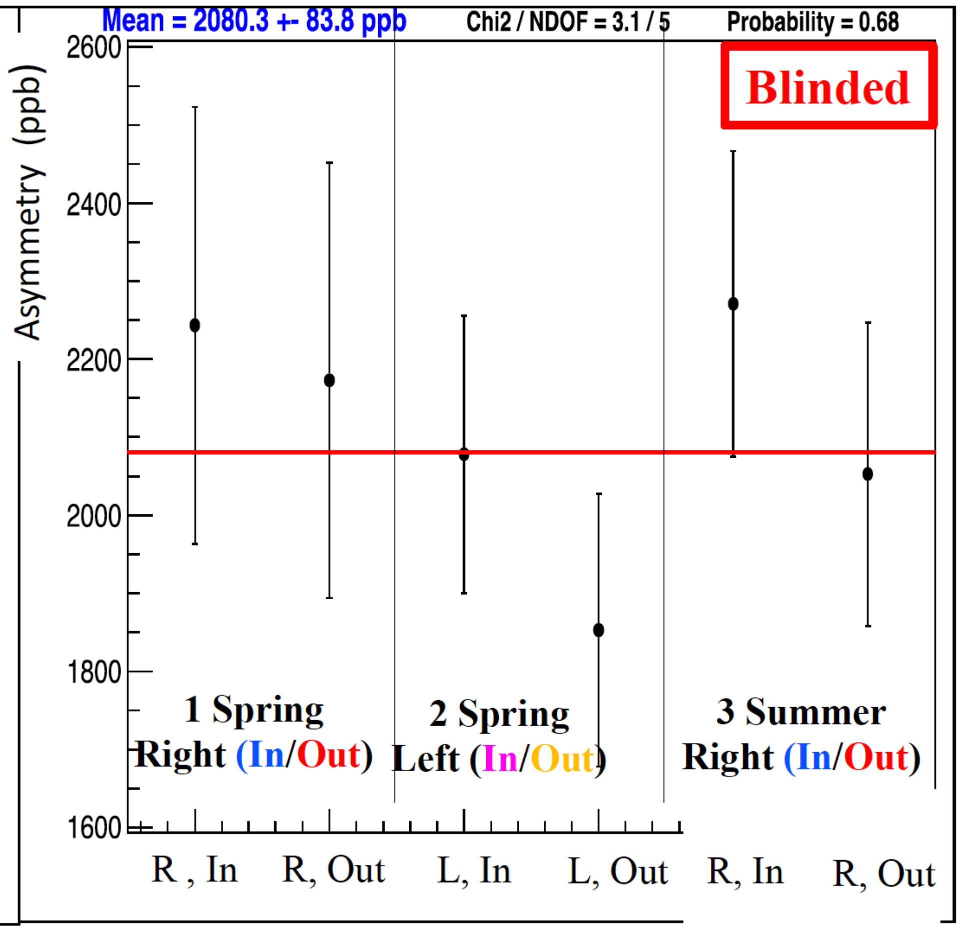

$$A_{PV} = R_{acceptNorm}\frac{A_{corr}/P_e - \sum_i A_i f_i}{1 - \sum_i f_i}$$

$$A_{corr} = A_{raw} + A_{beam} + A_{nonLin} - A_{blind}$$

- corrected asymmetry removed effects from beam asymmetries and noise
- Blinded Apv
  - 2334.8 ± 106.1(stat) ± 37.3(sys) ppb

CREX Result

Unblinded on October 9, 2021

Unblinded APV:
2658.6 ± 113.2 ppb (4.3%)

<Q2> =0.0297+-0.0002 GeV^2

Presented at the DNP2021
by Caryn Palatchi on Oct 12.

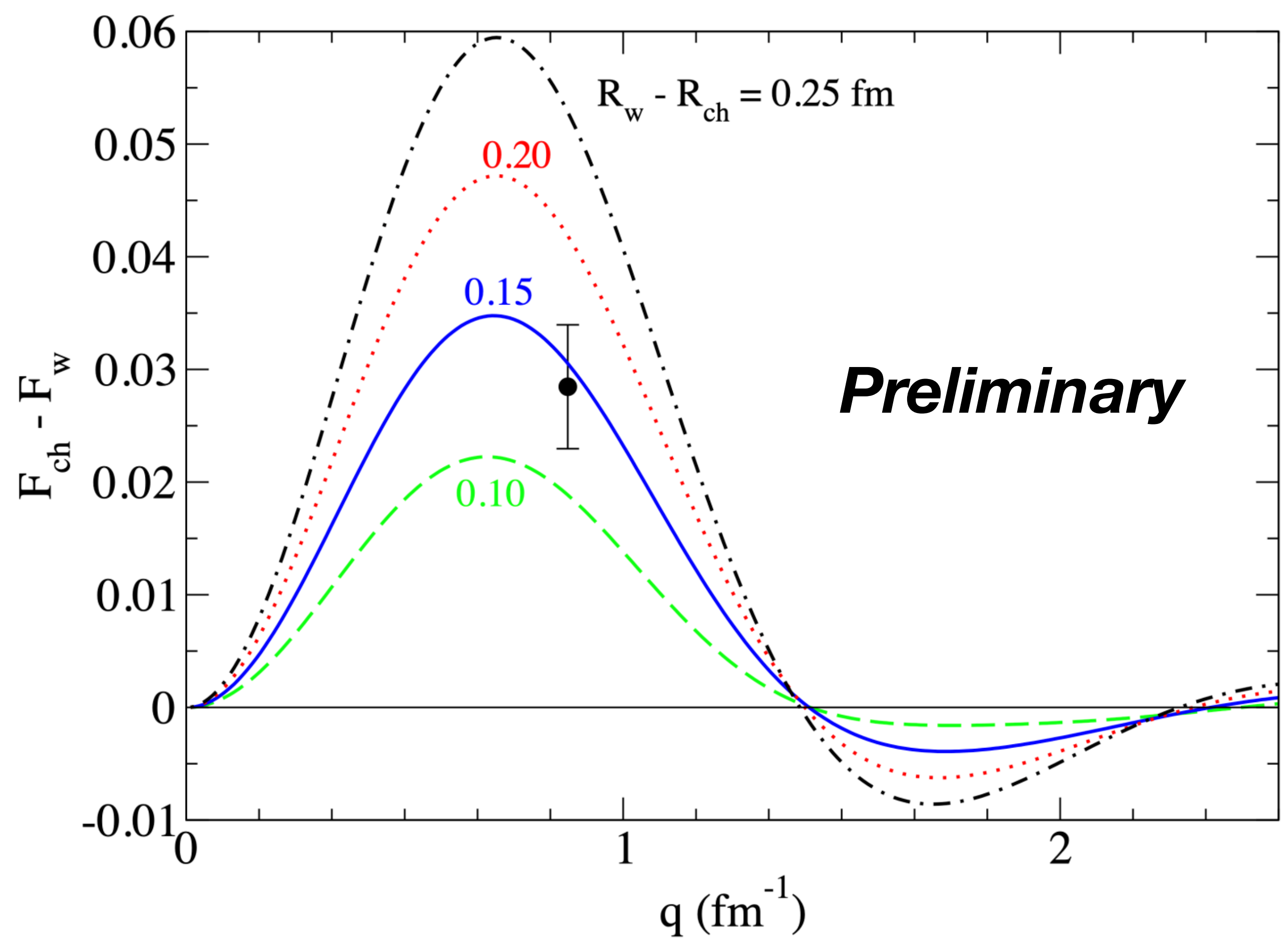

- Preliminary extraction of weak Form factor: F_W: 0.1297 ± 4.3%
- Analysis and extraction of neutron skin is ongoing

Collaboration

Spokespeople: Kent Paschke (contact), Krishna Kumar, Robert Michaels, Paul A. Souder, Guido M. Urciuoli

Post-docs and Run Coordinators: Rakitha Beminiwattha, Juan Carlos Cornejo, Mark-Macrae Dalton, Ciprian Gal, Chandan Ghosh, Donald Jones, Tyler Kutz, Hanjie Liu, Juliette Mammei, Dustin McNulty, Caryn Palatchi, Sanghwa Park, Ye Tian, Jinlong Zhang

Students: Devi Adhikari, Devaki Bhatta Pathak, Quinn Campagna, Yufan Chen, Cameron Clarke, Catherine Feldman, Iris Halilovic, Siyu Jian, Eric King, Carrington Metts, Marisa Petrusky, Amali Premathilake, Victoria Owen, Robert Radloff, Sakib Rahman, Ryan Richards, Ezekiel Wertz, Tao Ye, Allison Zec, Weibin Zhang

Thanks to the Hall A techs, Machine Control, Yves Roblin, Jay Benesch and other Jefferson Lab staff

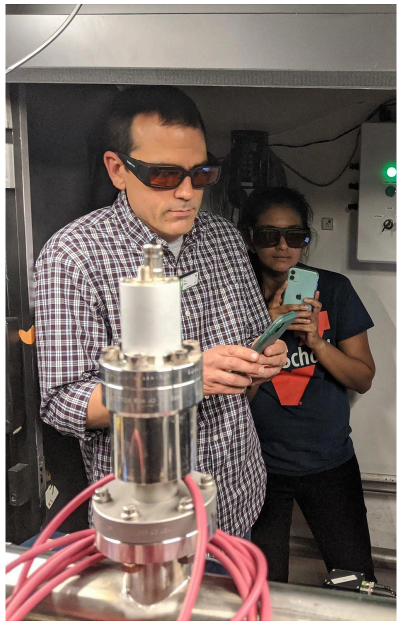

Summary

- PREX-2 successfully ran a technically difficult experiment
  - Significant neutron skin is determined from PREX A_{PV} , 0.283 (0.071) fm
  - Prefer to a larger L and larger neutron star
  - The final results were published in PRL as cover article in April 2021 and are already having an impact well beyond electron scattering community
- CREX just released the preliminary results for the asymmetry, theoretical implication is ongoing.
  - provide tests of DFTs and microscopic calculations and thus provide valuable new insight into nuclear structure

Summary

- PREX-2 successfully ran a technically difficult experiment
  - Significant neutron skin is determined from PREX A_{PV} , 0.283 (0.071) fm
  - Prefer to a larger L and larger neutron star
  - The final results were published in PRL as cover article in April 2021 and are already having an impact well beyond electron scattering community
- CREX just released the preliminary results for the asymmetry, theoretical implication is ongoing.
  - provide tests of DFTs and microscopic calculations and thus provide valuable new insight into nuclear structure

Thank you for your attention!

Backup

PREX-I (2010)

- Collected data at 2010
- 1.063 GeV electrons scattering from ^{208}Pb at 5 degree
- Initial goal: 3% precision

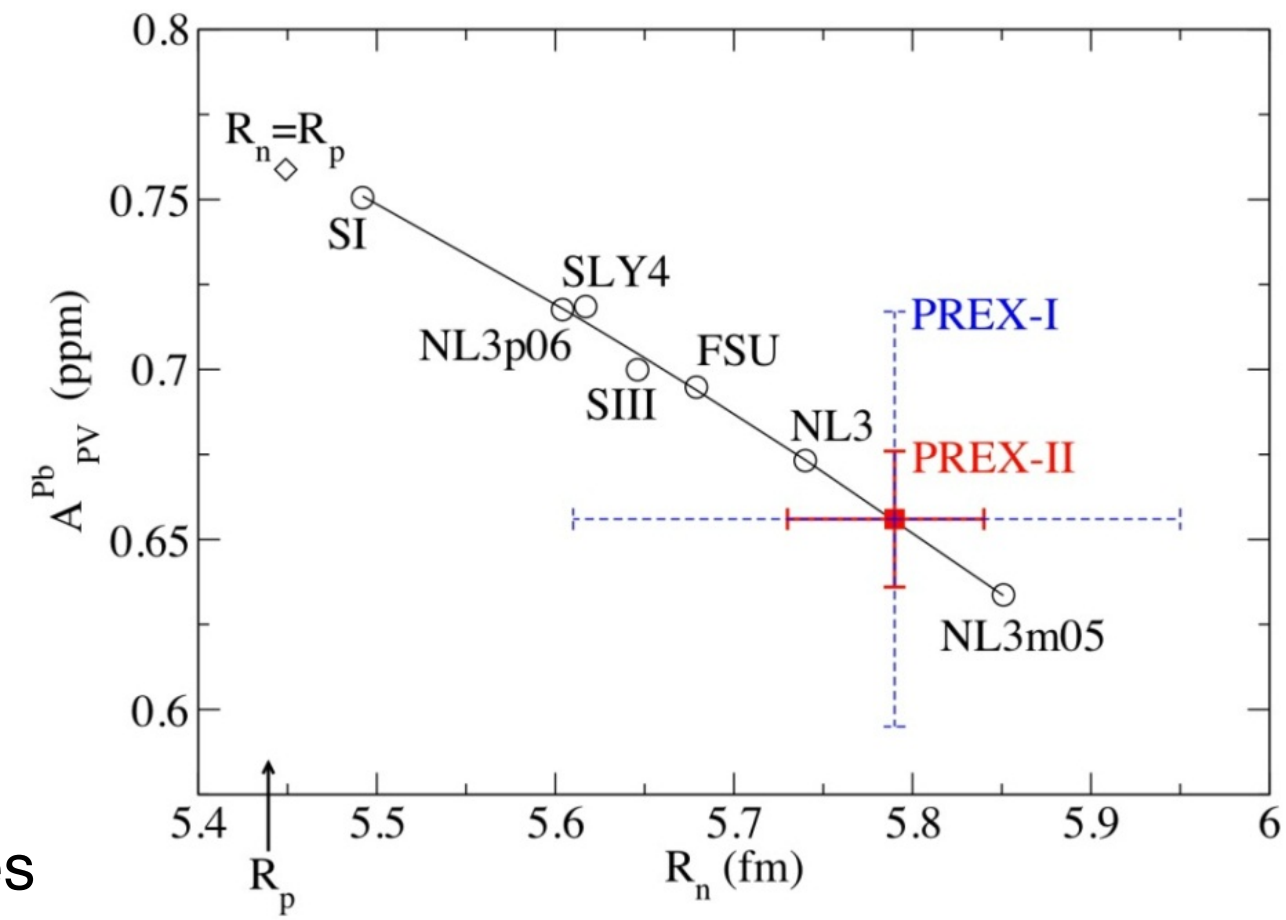

- Systematic uncertainties were well under control, however radiation issues limited the statistical uncertainty

A_{PV} = 0.657 ± 0.060(stat) ± 0.014(syst) ppm

First electroweak observation that there is a neutron skin around a heavy nucleus

$$R_n - R_p = 0.33^{+0.16}_{-0.18} \text{ fm}$$

Precision of PREX-I did not allow to exclude many models, motivation for PREX-II.

Neutron Star

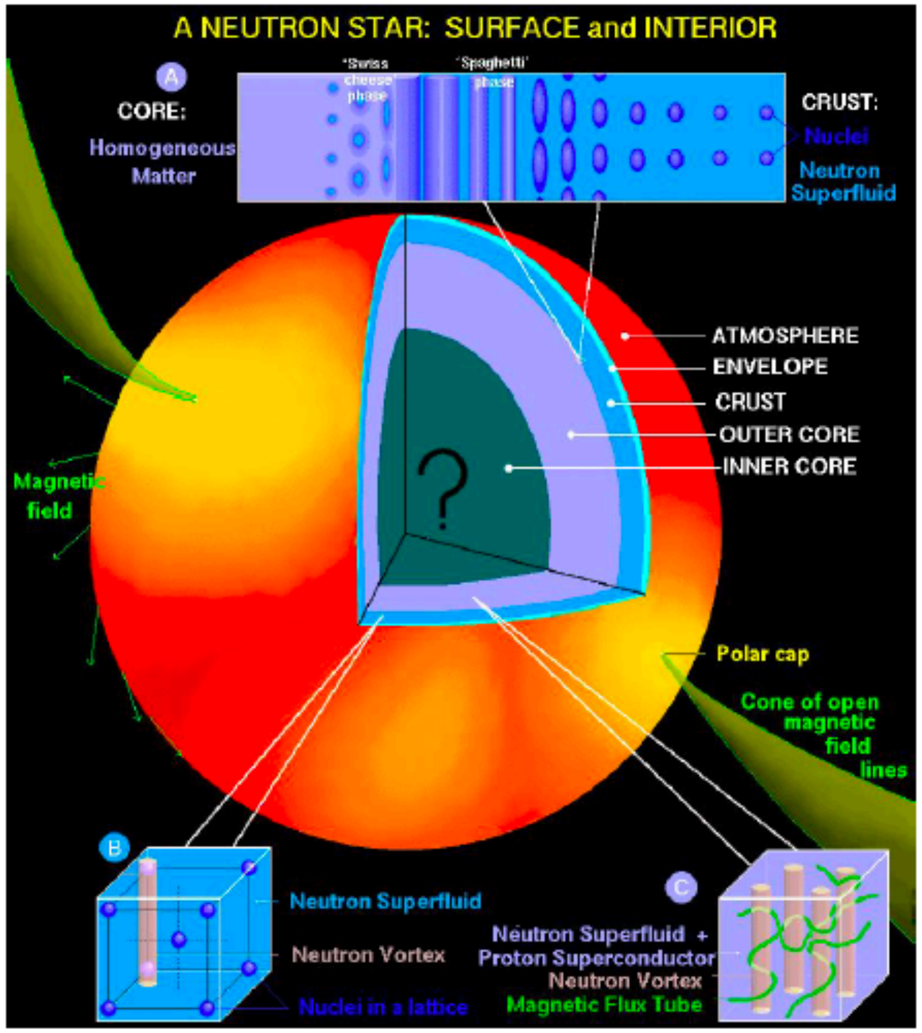

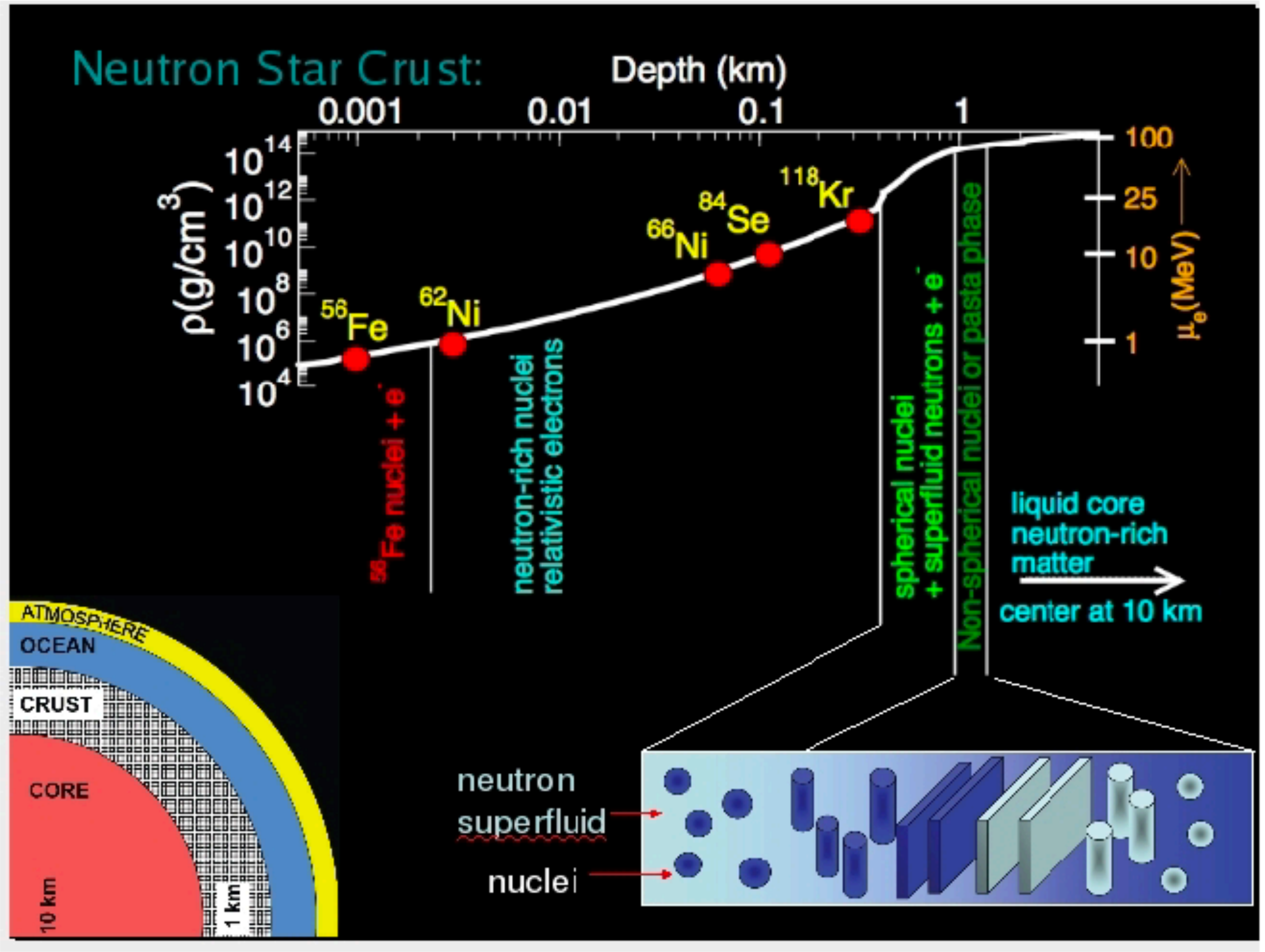

Nuclear Equation of State

At 0 temperature:

$$\mathcal{E}(\rho,\alpha) = \mathcal{E}_{\rm SNM}(\rho) + \alpha^2 \mathcal{S}(\rho) + \mathcal{O}(\alpha^4)$$

EOS can be written as expansion around symmetric limit of the energy per nucleon

$$\alpha \equiv (\rho_n - \rho_p)/(\rho_n + \rho_p)$$

$$\mathcal{S}(\rho) \approx \mathcal{E}(\rho, \alpha=1) - \mathcal{E}(\rho, \alpha=0)$$

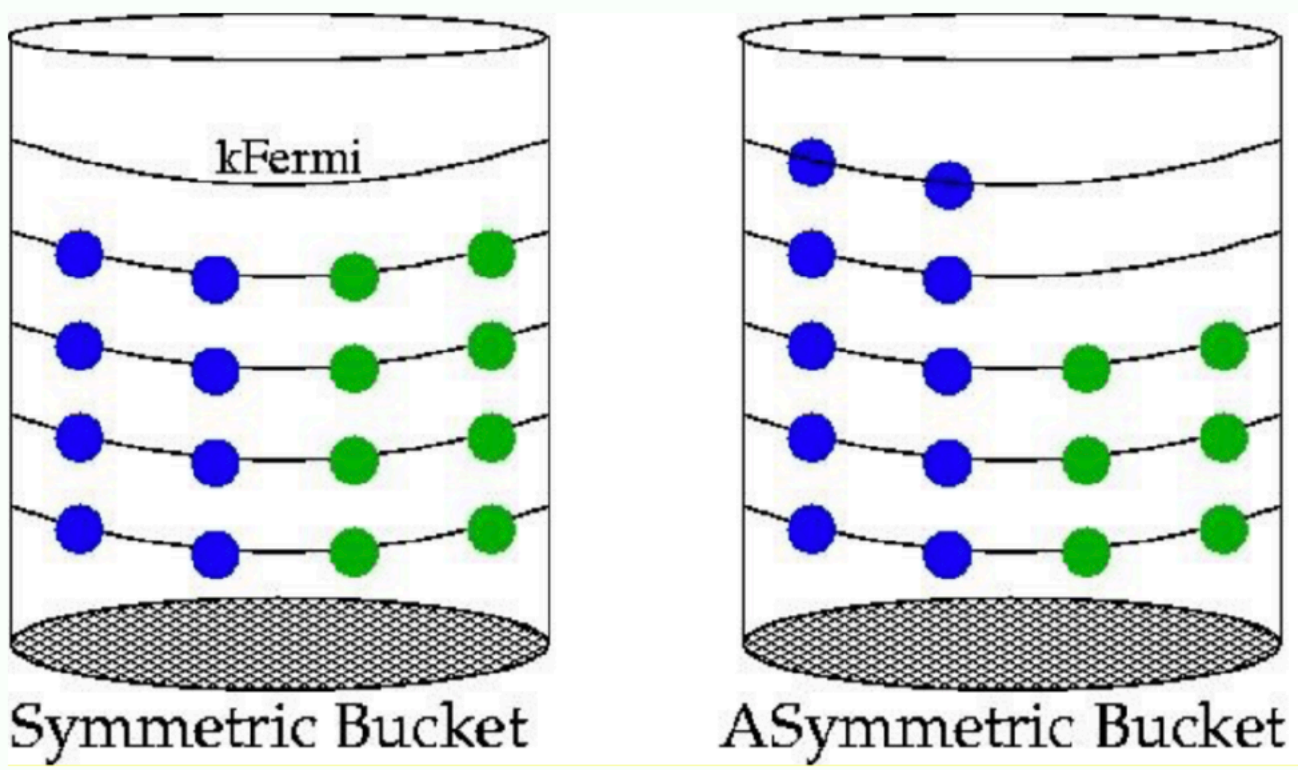

Taylor series expansion around saturation density:

$$\mathcal{E}_{\rm SNM}(\rho) = \varepsilon_0 + \frac{1}{2} K_0 x^2 + \ldots$$

$$x = (\rho - \rho_0)/3\rho_0$$

Energy per nucleon

Incompressibility coefficient

Symmetry Energy

$$\mathcal{E}_{\rm SNM}(\rho) = \varepsilon_0 + \frac{1}{2}K_0 x^2 + \ldots,$$

$$\mathcal{S}(\rho) = J + Lx + \frac{1}{2}K_{\rm sym}x^2 + \ldots,$$

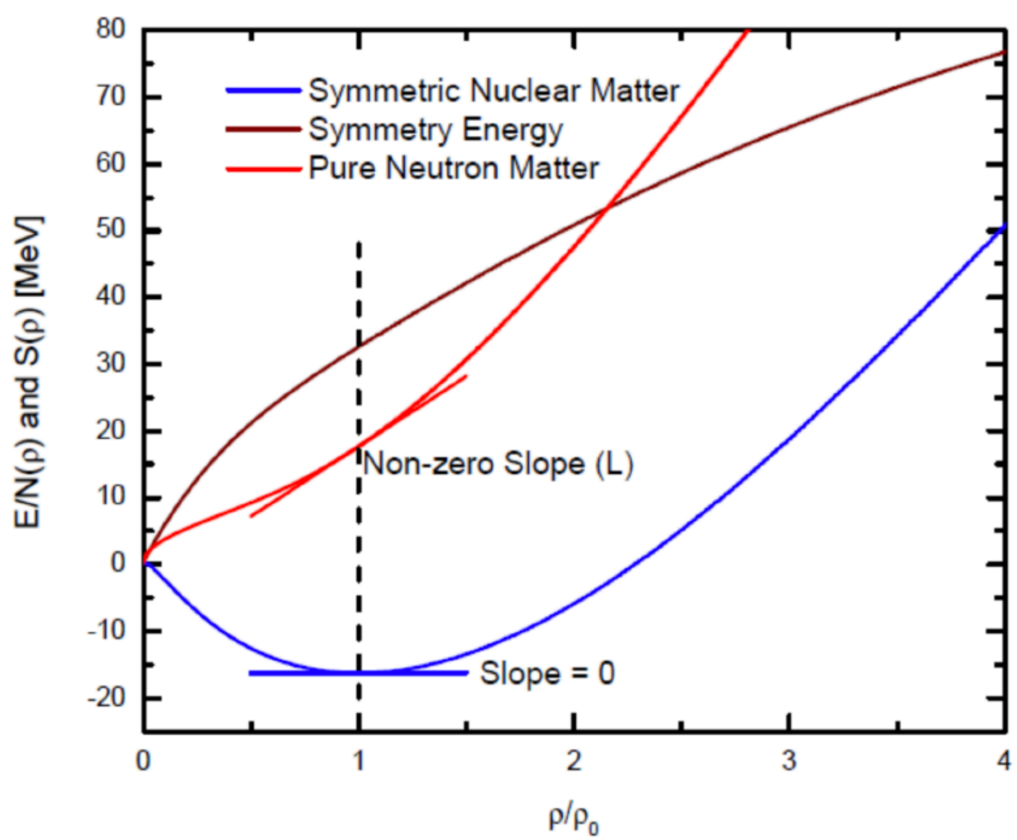

Pressure of pure neutron matter at saturation density:

$$P_0 \approx \frac{1}{3}\rho_0 L$$

- Nuclear masses are largely insensitive to the density dependence of the symmetry energy
- The extent of the neutron skin in a neutron rich nucleus is the result of balance between the surface tension and the slope of the symmetry energy
- The slope can be obtained by looking at the difference in the symmetry energy between:
  - The inner core (SNM at saturation density)
  - The outer core (lower nuclear densities)

Parity Violation in high energy scattering

Longitudinal single spin asymmetry

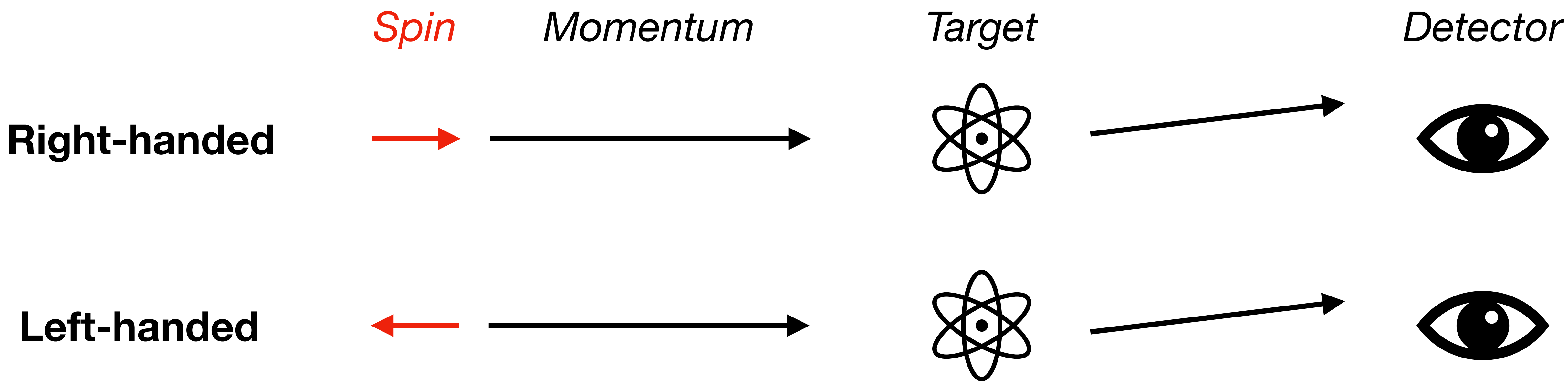

砷化镓GaAs光电子源

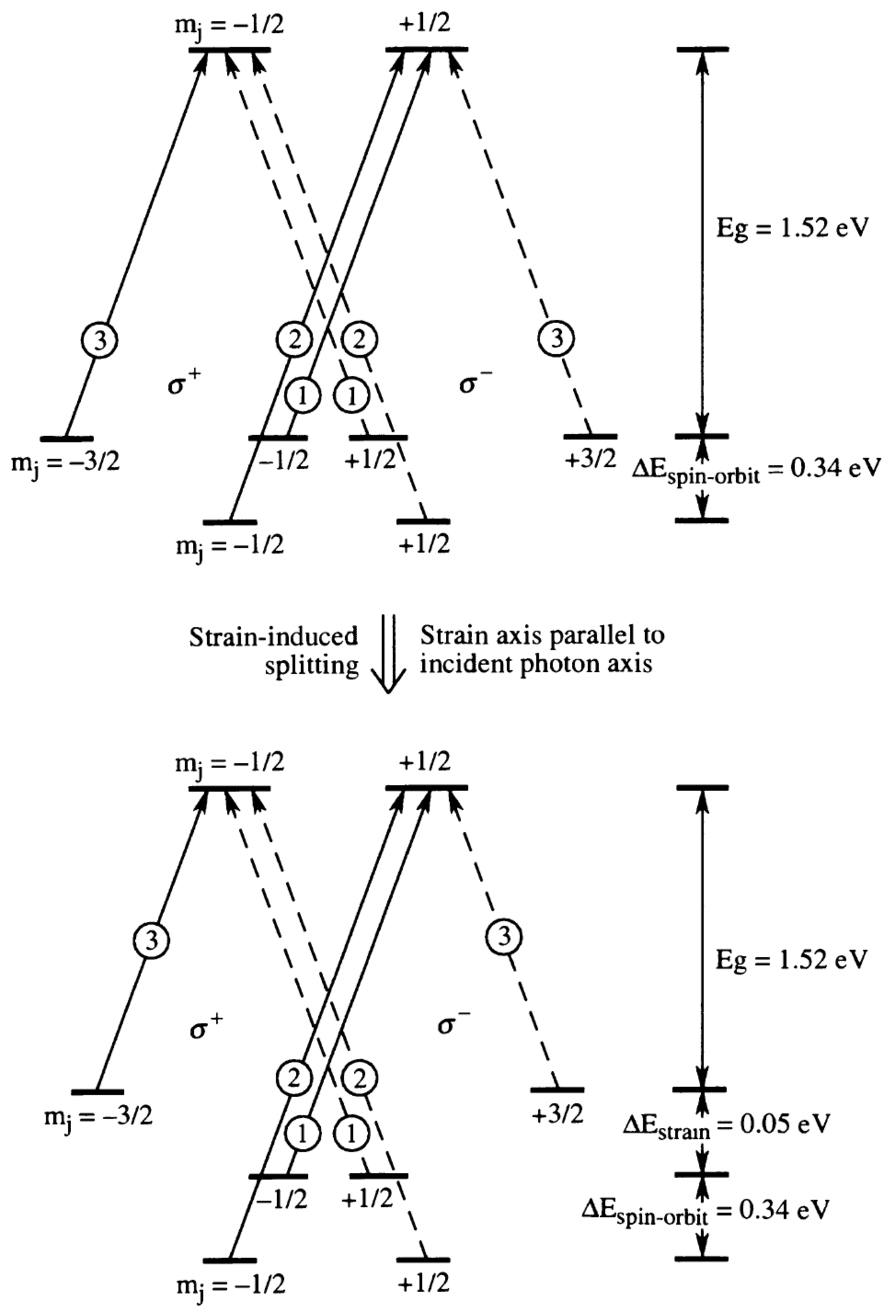

- 在圆偏振光激发下，电子从价带$p_{3/2}$和$p_{1/2}$ 跃迁到导带$s_{1/2}$
- 控制激光能量:
  $$E_g \leq \hbar\omega \leq E_g + \Delta E_{spin-orbit}$$
  - 极化度：(3-1)/(3+1) = 50%
- 砷化镓表面镀Cs_2O，形成负电子亲和势（NEA），受激极化电子发射

- 砷化镓晶体应变生长，$p_{3/2}$ 能级简并消除
- $E_g + \Delta E_{strain} \leq \hbar\omega \leq E_g + \Delta E_{spin-orbit}$
- 极化度： 100%